Perspective on Integrative Simulations of Bioenergetic Domains

Mohammad Mehdi Pirnia,[†] Ranel Maqdisi,[†] Sumit Mittal,[‡] Melih Sener,^{†,¶} and Abhishek Singharoy*,[†]

†School of Molecular Sciences, Arizona State University, Tempe, United States ‡VIT Bhopal University, Sehore, Madhya Pradesh, India ¶Beckman Institute, University of Illinois at Urbana-Champaign

E-mail: asingharoy@asu.edu

Abstract

Bioenergetic processes in cells, such as photosynthesis or respiration, integrate so many time and length scales that they hinder the simulation of energy conversion with a mere single level of theory. Just like the myriad of experimental techniques required to examine each level of organization, an array of overlapping computational techniques are necessary to model energy conversion. Here, a perspective is presented on recent efforts for modeling bioenergetic phenomena with focus on molecular dynamics simulations and its variants as a primary method. An overview of the various classical, quantum mechanical, enhanced sampling, coarse-grained, Brownian dynamics, and Monte-Carlo methods is presented. Example applications discussed include multiscale simulations of membrane-wide electron transport, rate kinetics of ATP turnover from electrochemical gradients and finally, integrative modeling of the chromatophore, a photosynthetic pseudo-organelle.

Introduction

Biological energy transfer is central to all life on earth. Living cells can be considered as engines producing work while transferring energy between a source and a sink. However, delineating the mechanisms of energy storage and directional transfer is nontrivial due to the complexities associated with monitoring coupled reactions in confined and/or crowded environments. Molecular dynamics (MD)* of such processes often entails simulating a network of stochastic events under deterministic constraints, and sometimes the converse. We ground this perspective on such integrative or so-called multiscale approaches for studying the emergence of directional energy changes in bioenergetic membranes.

Historically, the areas of photosynthesis and mitochondrial respiration have offered a test bed for studying energy transfer in primitive organisms, plant and animal cells. These investigations have opened application areas in artificial light harvesting,⁵ biomarkers for cardiovascular diseases and cancer cells^{6,7} and more recently in brain sciences.⁸ One of the

^{*}Abbreviations: BChl: bacteriochlorophyll; Chl: chlorophyll; cyt: cytochrome; CpHMD: constant pH molecular dynamics; MC: Monte Carlo; MD: molecular dynamics; PSI/PSII: photosystem I/II; QM/MM: quantum mechanics/molecular mechanics; RC: reaction center; SMD: steered MD

first breakthroughs in understanding how energy is transfered in biology came from the discovery of *chemiosmotic coupling*. It described how electrochemical gradients can be employed to store energy in cells by the use of light- or nutrients-driven ion pumps. ⁹ Soon after, the notion of *chemomechanical coupling* was explored. It explains how these ion gradients are utilized to drive chemical reactions of metabolites by controlling directed movements of the proteins. ¹⁰ Efficiency of forward versus backward chemo-mechanical movements depends on the flexibility of the proteins. Finally, the directionality of the chemo-osmotic and chemo-mechanical cycles is contingent on the availability of the metabolites, which highlights the need for metabolite-carrier enzymes. ¹¹

The activity of the carrier proteins can be regulated even to reverse the cycles by changing the metabolite concentration and, hence, bias the direction of the protein movements. This reversibility underscores a mechanism often used for robust functioning across stresses. So a simple model of energy metabolism will encompass metabolite regulation, electrochemical gradient and chemo-mechanical changes. Examples of such bioenergetic mechanisms can be seen in different variants of the so-called electron transport chain, ¹² rotatory catalysis ¹³ and Warburg effect. ¹⁴

Many researchers, including ourselves have conceived a number of top-down and bottom-up approaches for multiscale modeling of energy conversion and transport processes. Presented in this work (Table 1) is a representative list of computational models made over the last two decades, which includes the simulations of light-harvesting, charge transfer, and associated diffusive and conformational transition steps. Some essential reviews of the systems biology oriented approaches in studying bioenergetics are provided elsewhere. ^{15,16} Presently, we focus on the detailed molecular simulations for studying biological energy transfer.

The organization of this manuscript is as follows. In the next section, computational methods for integrating energy conversion processes are discussed in terms of their advantages and shortcomings. Subsequently, some exemplary studies that employ such methods are reviewed. Lastly, future outlook for integrative simulations is discussed.

A survey of integrative simulation methods

Computational chemistry has evolved into an indispensable tool for the routine investigation of bioenergetic systems.¹⁷ These methods have provided details of the electronic and molecular structural changes that underpin reaction mechanisms, energetics, and dynamics of proteins ranging from antenna complexes ¹⁸ to soluble charge carriers, ¹⁹ up to redox-driven pumps ²⁰ and to ATP driven motors. ^{10,21} Thus, it is possible to simultaneously investigate both conformationally-coupled charge transitions and diffusive transformations that underlie energy transfer networks. Here, we briefly discuss the development, application and challenges of popular methods sampled from Table 1 with an emphasis on those interfacing MD simulations.

Classical molecular dynamics simulations:

Conformational dynamics of a system can be assessed through MD simulation. ^{22,23} In this approach, every atom of the system, including the macromolecules (proteins, nucleic acids, cofactors), membrane, and the explicit solvent surrounding them is modeled using Newton's Second Law by integrating over energy functions called force field parameters. With the inception of customized hardware, ^{24–28} there has been a dramatic growth in the system-size and complexity handled by MD, which reflects in the area of bioenergetics (Fig. 1). MD offers an ideal tool for the visualization of sub-nanosecond collective phenomena, such as excitation transfer events . ^{29,30} In particular, the explicit modeling of lipid bilayers and membrane-protein systems lends to an accurate description of thermal disorder for computing the efficiency of light absorption by antenna complexes. ³¹

A well-known shortcoming of MD simulations stems from inability to access larger system sizes³² and longer time-scales.³³ Additionally, the lack of polarizable force fields for the related cofactors hinders quantitative estimation of long-range spatial information transfer even over short timescales.^{34,35} The sub-microseconds timescale accessible in MD for the nanoscale bioenergetic complexes that are typically 300 KDa to 1000 KDa in weight remain several orders of magnitude smaller than those probed by microscopy or imaging experiments and even smaller than those needed to study diffusive energy transfer.

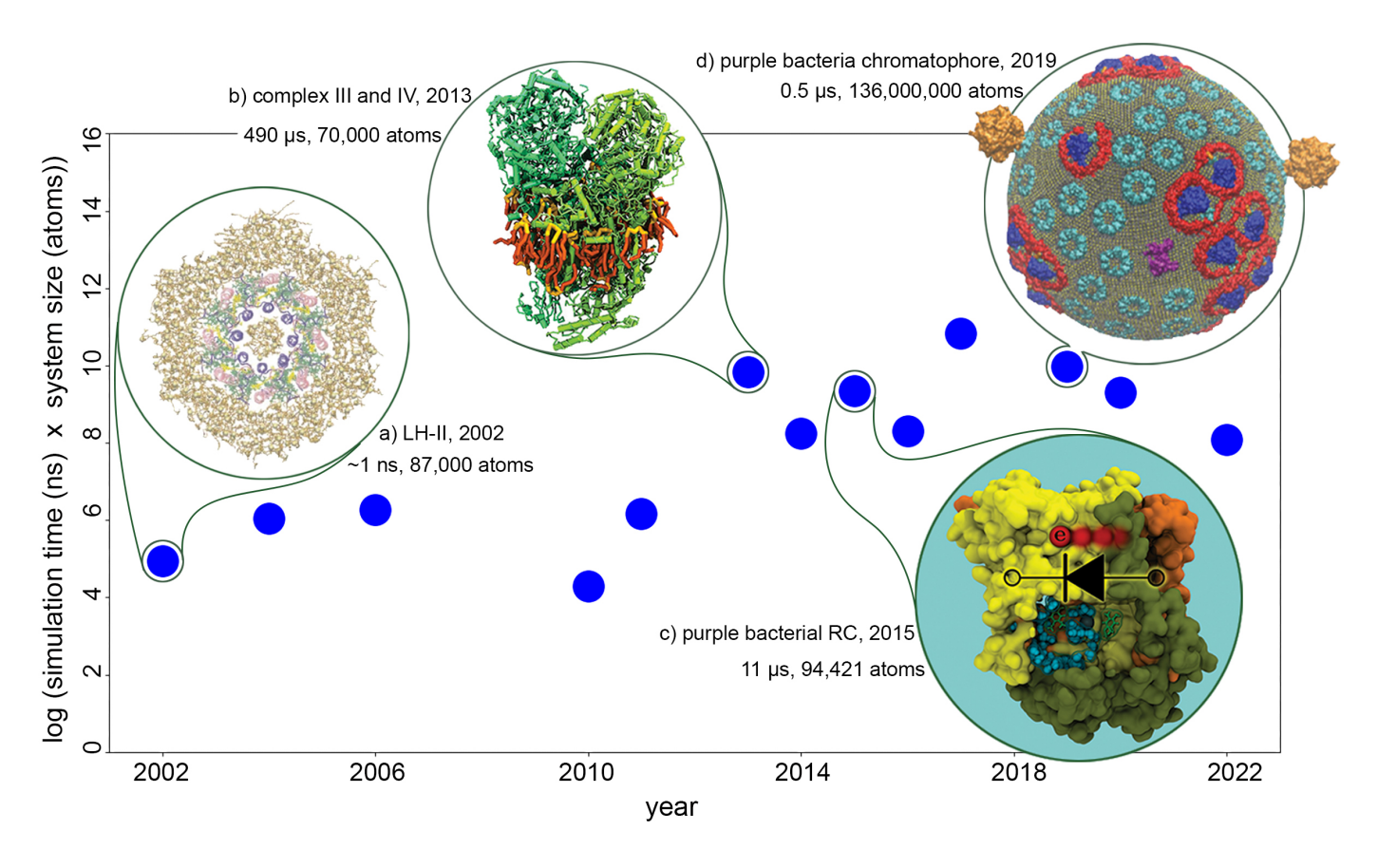


Figure 1: Significant bioenergetics MD simulations in the last couple of decades. The Y-axis describes computational expense in terms of a logarithmic scale of the simulation length multiplied by the atom number of each system. Four simulations with thumbnails displaying their simulated biomolecular structure, are pioneering works; a) the first MD simulation of a bioenergetic complex with a computational expense as big as ~ 85 kiloatom nanoseceond, b) the longest course grained MD simulation of a bioenergetic system, c) the longest all-atom MD simulation on a bioenergetic system, and d) the largest simulated bioenergetic system with 136 million atoms.

Another restriction of conventional MD simulation in bioenergetics is that the chemical state (e.g. redox or protonation) of all residues and cofactors is predefined and kept fixed throughout the simulation.³⁴ Pigment molecules are parameterized and their force fields are additively extended for potentially every new species-specific substitution to the cofactors (Fig. 2), which sometimes requires weeks to months of multi-dimensional fitting.³⁶ Despite this laborous stage in the set up, MD simulations at best sample only those molecular structures aligning with the most probable region in the harmonic potential. The chemistry of the system, which evolves with the conformations is overlooked. Simultanious computation of mechanical and chemical changes warrants the inclusion of the electronic degrees of freedom in MD, particularly for the computations of bioenergetic chemical gradients.³⁷ To this end, augmentations to MD are made either semi-classically (e.g. via CpHMD schemes) or quantum mechanically by introducing multi-physics computations.^{38–40}

Quantum Mechanics/Molecular Mechanics:

Quantum mechanical (QM) calculations provide electronic structure information of a molecule by solving the Schrödinger equation for all interacting electrons in the field generated by the nuclei. Reviewed in, 41,42 single or multi-reference QM methods, such as Density Functional Theory (DFT), configuration interaction (CI), 43 or couple cluster (CC) provide description of the ground-state energy of a molecule with different levels of accuracy, but are often limited to less than 100 atoms due to complexities that arise from the increasing number of atoms. The photosynthetic chromophores require an robust description of the excited electronic states in addition to their ground state. Time-dependent analogue of the DFT has provided an accurate description of these states, offering insights into properties such as excitation energies and polarizability. 44,45 The combination of DFT with multi-reference configuration interaction (DFT/MRCI), is also used to study excited states of a system. 46,47

Photosynthetic systems further require an accurate description of the dispersion interactions to account for exciton migration, and interactions between pigments and protein residues. Hence, DFT calculations have been refined to include the dispersion forces, commonly known as Dispersion-Corrected DFT. ⁵¹ More accurate methods, such as DFT + many-body dispersion, are also available, and go beyond the pairwise dispersion corrections to

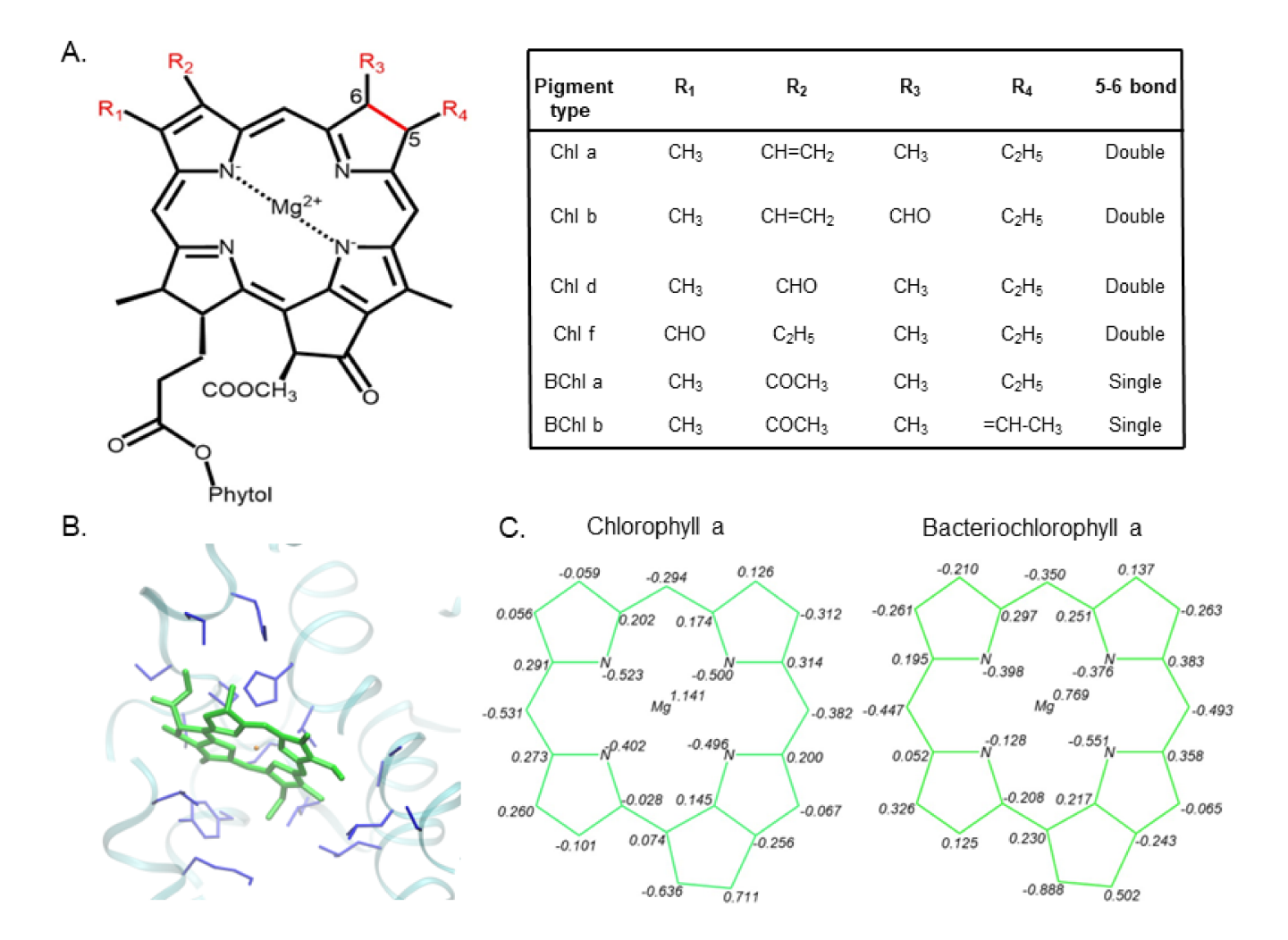


Figure 2: Biological chlorophyll a type pigments. (A) Chemical diversity of the chlorophyll porphyrin scaffold. Red colored components correspond to functional groups that distinguish the select group of pigment types designated in the table. (B) Truncated chlorophyll molecule (in green), taken from crystal structure (PDB:6NWA), ⁴⁸ shown ensconced in a protein environment (backbone in teal, sidechains in blue) that tunes its energetic properties dynamically. Visualization was done with VMD with the chlorophyll and protein sidechains rendered in licorice, and protein backbone in ribbon. (C) Side by side comparison of electrostatic partial charges for the chlorophyll a ⁴⁹ and BChl a ⁵⁰ atoms in the porphyrin skeleton (in green) determined via quantum mechanical calculations.

include higher-order terms to account for many-body effects.⁵²

The effect of the protein and environment has to be included, given the electronic structure has a very strong parametric dependence on the so-called bath variables. To study multiscale processes, QM/MM hybrid method is employed, in which a quantum mechanical description is embedded in a molecular mechanics environment.⁵³ Semi-empirical methods enable large QM region, longer simulations,⁵⁴ and have been parameterized against absorption and circular dichroism spectra of pigments. As such, methods like AM1, PM3 up to PM6 have successfully been coupled with classical CHARMM or Amber force fields within light harvesting systems to study the broad absorption spectra of bacteriochlorophyll rings. ^{18,55}

Finally, the presence of open shell electronic structure in bioenergetic systems such as charge-separated chlorophylls, semi-quinones or reactive oxygen species, pose a challenge to routinely used DFT functionals. ⁵⁶ These systems may suffer from spin contamination due to the lack of a spin adaption description. In the modern architecture of QM, several variants of MRCI or MRCC have been developed to provide a reasonable description of open-shell species. ^{44,57,58} Density-fitting approaches and local correlation methods have also been developed, which may be applicable for medium-sized (150-200 atoms) systems. ⁵⁹ Examples of such methods include DFT with broken symmetry ⁶⁰ and the Tao-Perdew-Staroverov-Scuseria functional. ⁶¹ The latter is a so called meta-GGA functional combining exchange and correlation terms with additional gradients of the electron density, and has been used to study metal centers such as [4Fe–4S] cluster in diphosphate reductase IspH protein and metalloproteins. ⁶²

Enhanced Sampling Methods:

Bioenergetic systems undergo large-scale structural transformations and reassembly processes in response to cellular stresses. Motor-like protein complexes, such as NADH dehydrogenase or ATP synthase undergo directional movements that is tuned by the direction of osmolyte fluxes (quinones, ADP, ATP, NADPH) across the membrane. To model these processes, it is crucial to generate an ensemble of the transient conformations, classify them in a physically interpretable yet 'reduced space' of reaction coordinate(s), and pinpoint the interactions that act as rate-determining bottlenecks in the structure and energy cascades.

Although a few microseconds of MD simulations are routine now, the resulting ensemble of structures might not conform to the ergodicity principle, requiring more exhaustive sampling of the conformational space.

Several enhanced sampling simulation algorithms have been developed to improve the description of thermodynamic ensembles within reasonable computing resources. ^{63,64} These methods aim to capture lower probability regions on the potential energy surface that are associated with high-energy barriers. Two broad categories of methods have emerged, important or biased sampling and generalized sampling. While the former requires a priori information of the reaction coordinates, along which the ensembles are generated, the latter family of methods do not need any such dimensionality reduction.

Given the amenability to work with large system sizes, biased sampling methods have been quite popular in simulations of bioenergetic complexes. ^{65–67} For starters, steered MD or SMD simulations have been used extensively to study such systems. This type of simulations have provided initial insights on binding and dissociation events of electron carriers. For example, the *Rhodobacter sphaeroides*'s RC complex reduces a quinone to semiquinone upon receiving electron from its core protein. An experimental study observed a significant difference in the dissociation of the neutral and anionic quinone at their binding site. ⁶⁸ Then SMD simulations were used to dissect the mechanistic differences of the reduced and oxidized quinone binding. ⁶⁹ Similar studies have also been utilized to study redox protein binding to the respiratory complexes. ⁷⁰ However, such simulations are highly driven by the investigators' intuition and often fail to capture movements orthogonal to the direction of steering ^{71,72} leading to the inception of more sophisticated importance sampling tools.

Metadynamics improves conformational sampling by discouraging the simulation to visit previously sampled states. ^{73,74}These simulations have successfully modeled protein-protein dissociation events or rearrangement of cofactors at different binding sites, ^{75,76} resolving some of the slowest steps in bioenergetic processes and elucidating the properties of the dissociated state. ^{77–79} A major advantage of metadynamics over other free energy methods is that, provided the knowledge of putative reaction coordinates, the free energy profile can be extracted from the accumulated bias potential without requiring separate simulation for each state.

Another common method for enhance sampling along a predefined reaction coordinate is *umbrella sampling*. A harmonic potential is employed to improve the sampling points along the reaction coordinate of a transformation, which is discretized by a series of windows. The relative free energy change of this transformation is determined by de-weighting this potential from all the windows. ⁶⁵

The major challenge with both metadynamics and umbrella sampling simulations is that these methods are limited to simultaneously handle only a few reduced degrees of freedom, also called collective variables (typically up to four). Not to mention, the lack of sampling other degrees of freedom aside from the chosen collective variables can produce misleading outcomes. The computational cost is further increased by the requirement of statistical methods, such as bootstrapping analysis, to quantify the convergence and uncertainty in the calculated free energy values. This issue is being overcome by integrating experimental data inside simulations of large protein complexes either as direct force field bias ⁸⁰ or as a probability bias ⁸¹ that focuses the enhanced MD sampling on relevant parts of the free energy landscape. ⁸²

Coarse grained modeling:

The all-atom MD simulations are generally limited to few tens of microseconds of time and few nanometers of system size. Coarse-grained (CG) MD simulations aim to capture larger-scale rearrangement of such systems by reducing the number of particles and interaction details, and thus increasing both accessible temporal and spatial scale without any significant increment in computational resources. ^{83,84} Coarse graining involves grouping of multiple atoms (3-6 non-hydrogen atoms) to form a single, larger particle, known as bead, and is based on the idea that not all atomic details are relevant for the dynamics and behaviour of the system can be averaged without much loss of important information. Still, brute force CG MD simulations are of limited use for studying systems where atomic-level interactions, such as hydrogen bond which are important for protein secondary structures, are crucial. Approaches are being developed that offer CG dynamics, yet with corrections that account for atomistic interactions, such as the multiscale force-matching ⁸⁵ or Upside. ⁸⁶

Simulations of bioenergetic systems were performed using CG MD to probe the slow

membrane dynamics, and the influence of diffusive lipid binding on the structure and function of integral membrane proteins. $^{19,87-89}$ Significantly reducing the number of particles, CG MD simulations have been performed in the range of a few hundred microseconds. 90 The primary challenge in studying bioenergetic systems using coarse graining is the accurate parameterization of the cofactors, such as chlorophyll a/b in photosystems. 91 Nonetheless, CG force field parameters for several cofactors involved in bioenergetics have been developed. In particular, the MARTINI force field, which is one of the most commonly used CG force fields, 92 has been extended for photosynthetic systems by developing parameters for its components, such as chlorophyll a/b, plastoquinone and β -carotene. 91,93 These parameters are based on values obtained from the corresponding all-atom simulations and are compatible with their partition coefficient in hydrated organic solvents, such as octanol/water, cyclohexane/water. The MARTINI simulations are also employed to study the formation of LHCII assembly and the dynamics of PS II cofactors embedded in the thylakoid membrane. 88,94

Other methods:

Monte Carlo simulation. As a versatile, non-MD sampling method, MC is used to explore the conformational and energy landscape of complex biomolecular systems, including the bioenergetic ones. During a standard MC simulation, a large number of random conformations of the system are generated by altering various structural features and an energy-based criterion, such as Metropolis, is used to direct the simulation to an energy minimum and provide statistical-relevant properties. In the context of bioenergetics, MC simulations are employed to study processes such as the reconfiguration of protein-protein interfaces on the organization of bioenergetic complexes, 95,96 or the influence of amino acid mutations on the interaction energies in photosystems. 20,97 Protein backbones are often kept fixed when the side chains are sampled. 98 Nonetheless, a recent study found that inclusion of protein-protein interactions during MC simulation increases the computational cost, but offers a more accurate description of the arrangement of photosynthetic proteins within the thylakoid membrane compared to single-particle MC simulation. 99 The limitation of slow convergence can be overcome by employing temperature replica exchange MC (t-REMC) method, 100,101 sometimes with solute tempering, 102,103

MC simulations are also being extended to investigate the electronic structure by the development of Quantum Monte Carlo (QMC) simulations.¹⁰⁴ These simulations can be used to study the electronic structure of ground and excited states with thousands of electrons as well as the electron transfer pathway and are highly useful to study bioenergetic systems and processes.^{105,106} Moroever, QMC simulations have been used to study light absorption and energy transfer by photosynthetic pigments in light harvesting complexes of higher plants.¹⁰⁷

Constant pH simulation. The effects of different pH conditions on the dynamics of a system can be studied by CpHMD simulations. ¹⁰⁸ The strength of these methods lies in their ability to sample various protonation states of residues and other ionizable groups during the course of the simulation trajectory. This opens the door for assessing relationships between ionization states of different groups inside a biomolecule and the structural and functional properties of the system, such as stability and internal interactions respectively.

In the discrete CpHMD simulation, based on a hybrid MD/MC approach, ^{109,110} the ionizable residues of the system are initially assigned a specific protonation state according to the chosen pH value. Then, MD simulation is used to produce a trajectory to obtain possible configurations at which different redox states of the the stated residues are energetically allowed. Performing MC sampling, configurations at a specific time interval are selected from the MD trajectory, and the protonation state of each titratable residue is decided based on Metropolis criterion. ¹¹¹ For example, CpHMD simulation at six different pH values (from 3 to 8) were performed for PSII subunit S and the frequency of protonation for all titratable residues at each pH was determined. ¹¹² The protein was observed to undergo secondary structural changes depending on the pH value, primarily due to the change in the protonation states of multiple Glu residues. Similar studies have been performed for bioenergetic systems, such as light-harvesting complex stress-related of moss *Physcomitrella patens* and RC of *Rb. sphaeroides*, with a focus on determining their pH sensitivity. ^{113,114}

Brownian Dynamics or BD simulation. Diffusive transport of charge within the cellular medium via soluble proteins (cytochromes, ferredoxins or plastocyanins) is one of the key steps of biological energy transfer. Such long-range interactions play a crucial role in enabling the recognition of binding partners despite crowded environments. This step, which

occurs at a slower rate compared to conformational transitions, represents a rate-determining bottleneck, further challenging the limits of MD simulations.

In BD simulations, the environment is modeled as a mean field of electrostatic and van der Waals potential, wherein the atom-resolved binder proteins diffuse to mutually interact. ^{115–117} The statistics of binding conformations derived from these simulations are employed to delineate the key recognition motifs of the binders. A major advantage of this simulation is that it manages to overcome the entropic bottlenecks of MD simulations by sampling multiple binding and unbinding events within a finite compute time. The mean-field approximations allow even larger timesteps than CG simulations. However, the macromolecules are often treated as rigid bodies. Hence, despite capturing the interaction surface, mechanisms like induced fit are beyond the scope of these simulations. Hybrid methods switching between MD and BD have been proposed for studying the binding of ions to proteins to include the induced structural changes in proteins. ^{118,119}

Resulting applications

In this section, three exemplary applications are discussed that highlight the theory and simulation method for modeling molecular mechanisms of biological energy transfer. We will start with a summary of work on redox processes within the electron transport chain, continue to chemo-mechanically coupled conformational changes, and finally discuss an integrative model of light harvesting.

Electron transport chain:

The role of thermal disorder in sustaining long-range excitation transfer in light-harvesting complexes has been investigated using MD simulations. ¹²⁰ Following site-energy computations of the pigments, ⁵⁵ the Försters theory of excitation transfer is employed with a so-called effective Hamiltonian model to determine fluorescent resonant energy transfer in pigment-protein complexes of different architectures. ¹²¹ A remarkable result was that several dark states of low oscillator strength were found below the main Soret band for solvent complexes and chlorophylls and bacteriochlorophylls in the protein environment. ¹²² These states were

predicted to be intermediate states for excitation energy transfer in photosynthetic complexes, which was subsequently verified by two-dimensional electron spectroscopy. ¹²³ Further MD simulations of PSI and PSII revealed that the relative flexibility of the subunits, which can influence the photosynthesis regulation, is further controlled by exposure to the membrane and water environment. ^{88,124} It allowed to monitor the extent and time scales of geometrical deformations of pigment and protein residues at room temperatures. ¹²⁵ A comparison of the average distances and angles between the B850 BChls to those found in the crystal structure reveals an increased degree of dimerization within the B850 ring, as compared to the crystal structure.

Following light absorption, the next major step in energy harvesting is charge separation so the optical energy is converted to electrochemical energy for longer-time storage and transduction. Computations with TDDFT method (see Methods) using the quantum mechanics/molecular mechanics/polarizable continuum model (QM/MM/PCM) method offered a seminal insight on the role of aromatic amino acid residues in reducing the energy barrier for charge separation. For example, in the RC protein, Tyrosine residues near the accessory BChl drastically accelerates charge separation by overcoming the electron-hole interaction. ¹²⁶ The symmetry-breaking of the chlorophyll conformation further dictates the direction of the resulting electron transfer to membrane-bound charge carriers quinone species.

Studies have utilized MD simulations to probe the dynamics of RC molecules in the light-harvesting complex LH-II embedded in a lipid bilayer in an explicit water environment. These simulations shed light on the sequential dynamics of BChl and quinone molecules as well as the role of water molecules on their interactions. ⁵⁵ Since the timescale of quinone unbinding to proteins is intractable by MD, SMD simulations followed by umbrella sampling are employed to measure the energy required for removing a reduced quinone from the RC in the photosynthetic membrane, ⁶⁹ or from analogous quinone-reducing NADH-dehydrogenase complex in the mitochondrial membrane. ²⁰ The values were found to be quite varied between multiple systems, anywhere between the range of 4-12 kcal/mol.

The reduced quinone is ubiquitously shuttled to the bc_1 complex. Here, two electrons are abstracted to reintroduce the oxidized quinone back into the membrane. These abstracted electrons make way through the bc_1 into the heme groups of the soluble transport proteins

cyt. c/c_2 that diffuse back to the RC to complete the cyclic electron transfer. A combination of MD and Brownian Dynamics simulations have revealed the mechanisms of diffusion, attachment and detachment of cyt. c/c_2 between the bc_1^{127} and RC. A key finding in these studies, which has been verified by AFM and EPR measurements, is the redox-controlled electrostatic nature of cyt. A number of basic residues at the protein-protein interface were shown to switch conformation and modulate the the redox complementarity of the electron donor and acceptor sites. Upon the single-electron redox reaction, the charged residues at the interface rearrange, resulting in reduced flexibility compared to when the donor-acceptor complex contains two holes or electrons.

Electron transport from the quinone binding site to the cyt. c site within the bc₁ complex remains a mystery. The series of charge transfer reactions between different cofactors, known as the Q-cycle, involves reduction of a quinone to quinol, which diffuses to the cyt. bc₁ complex and is oxidized back to quinone releasing two electrons to cyt c₁ heme groups via proton-coupled electron transfers reactions. ¹³⁰ Insights into these charge transfer reactions have been gained through MD simulations and QM calculations. ^{131–133} One such study revealed the binding pathway of quinol to the bc₁ complex and assessed the influence of nearby residues on the electron transfer between quinol and Fe-S cluster. ¹³¹ Another study used microsecond MD simulations of the membrane-bound Rhodobacter sphaeroides's RC bacterium to understand the role of primary and secondary quinone in modulating electron-transfer across the two symmetrical RC. ⁵⁰ The study highlighted the effect of neighboring water on electron transfer between cofactors.

ATP synthase:

Two protons are pumped into the periplasmic space per reduction of one quinone molecule at the bc_1 , which contributes to the proton-gradient or proton motive force. Over the reduction of two quinones, and hence the release of four protons, an ATP is generated chemo-mechanically by the ATP synthase motor. This formation of ATP completes the entrapment of light energy from the photosystems into the synthesis of a P - O chemical bond. This last step has been a focus of intense molecular simulations for close to two decades now.

The motor complex is composed of two subsystems, a transmembrane and a soluble part, each of which can independently perform directional rotatory movements. The F-type ATP synthase is the most studied given its ubiquity among both aerobic and anaerobic lifeforms. This type of ATPases exist in the bacterial plasma membrane, the mitochondrial inner membrane, and the thylakoid membrane within chloroplasts. On the other hand, driven by an array of new structures, the evolutionarily linked vacuolar or V- and Archeal or A-type ATPases are also recently simulated.¹³⁴

Proton transport driving rotation of the transmembrane F_o domain was modeled revealing a coupled protonation/deprotonation of two conserved acidic residues, ASP. ²¹ An ancillary mathematical model suggested the feasibility of torque generation guided by this molecular mechanism. Remarkably, this work was performed when the complete structure of the proton channel (the a - subunit) across the F_o domain was not known. Only in the last decade, with the inception of near-atomic resolution structure of F_o and V_o motors, the enhanced sampling simulations of these systems are getting traction. ¹³⁵ A key discovery is that the proton-transport-driven rotation of an isolated F_o motor is random, while that of an isolated V_o motor remains inhibited. Furthermore, the classic half-channel picture of proton transport is gradually being updated. In the traditional view, one half-channel needed to be dewetted before the opening of the other half-channel on the opposite side of the membrane. This is being replaced by an alternate-access mechanism which is promoted by sidechain re-orientations that prevent energetically expensive channel opening and closing. ¹³⁶

The soluble F_1/V_1 domains has been the focus of some of the longest possible MD simulations, ¹³⁷ SMD simulations, ¹³⁸ and elastic models. ¹³⁹ These studies have revealed that protein flexibility is crucial for reducing the energy barrier in proton pumping or ATP hydrolysis-driven power-strokes in the rotor, which stationary structures cannot uncover. And yet, major contention remains on whether the clockwise or counter-clockwise movement of this motor is driven by the power-stokes using a local elastic storage unit or is it purely driven by diffusion a.k.a a Brownian Ratchet. ¹⁴⁰ A unified view is emerging, wherein the kinetics of the motor is controlled by the power-stroke, while the rotational direction is tuned by a ratcheting mechanism.

Integration of energy conversion from electronic to cell scales in purple photosynthetic bacteria:

Integration of time and length scales across interlocking processes provides a primary challenge in the study of bioenergetic processes in photosynthesis, both computationally and experimentally, as exemplified by studies of purple phototrophic bacteria. ^{31,141,142} These disparate length and time scales necessitate a combination of computational approaches for determining structure and function at atomic, supra-molecular, organelle, and cell levels of organization (Fig. 3). At the core of such integrative modeling approaches are atomic detail structural models based upon experimental data on the supramolecular organization of the bioenergetic domains. In the *Rhodobacter sphaeroides* the primary photosynthetic domain is organized as the so-called chromatophore, a spherical pseudo-organelle of 60 nm diameter comprising over a hundred proteins and up to around 3,000 bacteriochlorophylls (Bchls) (Fig. 3B). A sequence of atomic detail structural models of increasing complexity were built for the chromatophore ^{143–146} based on atomic force microscopy, ^{147,148} cryo-electron microscopy, ^{145,149} crystallography, ^{150–153} optical spectroscopy, ^{144,154} mass spectroscopy, ¹⁴⁵ and proteomics ^{155–157} data. These structural models provide the basis for a corresponding set of functional models for energy conversion.

Energy conversion in a photosynthetic domain such as the chromatophore begins with the electronic excitation transfer (picoseconds), which can be described in an effective Hamiltonian formulation (Fig. 3 E, F). ^{121,146,166} Exciton transfer to the RC initiates charge transfer events (microseconds) through the so-called electron transfer chain. ^{167–169} These two quantum mechanical processes of excitation and electron transfer are followed by classical diffusion processes (milliseconds) involving the migration of charge carriers between different energy conversion proteins. As a case in point, charge carriers in the chromatophore are cyt. c₂ and quinone/quinol (Fig. 3G). Such diffusion processes are often rate limiting to the overall energy conversion rate as is the case in the chromatophore. ^{146,157,170,171} MD simulations are particularly suitable to address these intermediary timescales where charge migration can be addressed as a classical process; ³¹ specifically, the spatial inhomogeneity of the photosynthetic domain can be taken into account in terms of its electrostatic in-

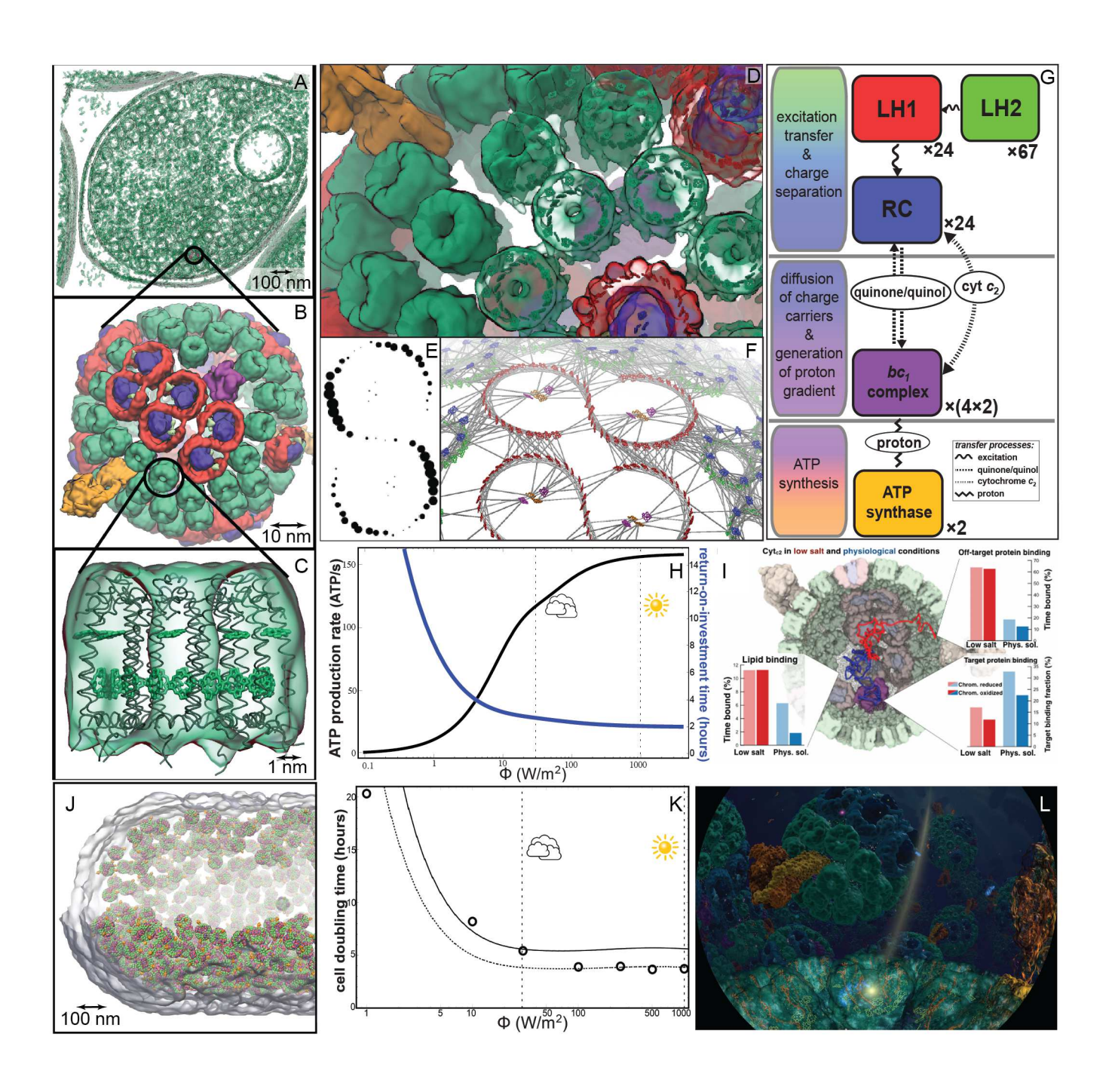


Figure 3: Determination of cell-scale observables 31,141,142,146 from structural and functional models of bioenergetic processes at atomic, protein, organelle, and cell levels. (A) Under low light-growth, the purple phototrophic bacterium R. sphaeroides expresses a dense network of hundreds of chromatophore vesicles for light-harvesting. ^{142,158} (B) Each of these vesicles, in turn, comprise hundreds of membrane-bound proteins, ^{143–146,159} primarily, LH2¹⁶⁰ (C; green) and LH1-RC¹⁶¹ (red-blue), cyt. bc_1 complex¹⁶² (purple), and ATP synthase^{10,163,164} (orange). The bacteriochlorophylls, represented in (D) as porphyrin rings, form an excitation transfer network described in an effective Hamiltonian formulation, ¹²¹ expressed in terms of electronic eigenstates ¹⁶¹ (E) and inter-pigment couplings ^{143,146} (F). (G) Excitation transfer is followed by the steps of charge carrier diffusion, proton-motive force generation, and ATP synthesis described in a multi-scale model for energy conversion. 31,142,146,158,159 (H) The ATP synthesis rate per chromatophore (black) 145,146 is computed as a function of illumination along with the corresponding return-on-investment time (blue), ¹⁴¹ i.e., the time for a chromatophore to produce enough ATP to pay for a copy of itself. (I) A 130 million atom MD simulation of the chromatophore³¹ determines the salinity dependence of the diffusion of cyt. c₂, a critical charge carrier in the energy conversion pathway. (J) Structural model of a low-light adapted cell¹⁴² featuring 985 chromatophores (non-chromatophore inclusion bodies absent) with size (1.6 μ m) and the radial distribution of chromatophores corresponding to cryoEM tomography data; 165 the model comprises a total of 2,431,965 BChls. (K) The doubling time of the bacterium (black line: computed, circles: experimental) is determined 141 from the return-on-investment time in (H) in terms of the time required for the entire cell to produce enough ATP, beyond base metabolism, to manufacture a whole new cell, reproducing, in particular, the low-light saturation behavior typical of R. sphaeroides. (L) The visualization techniques necessary for computational modeling through multiple scales also enable outreach narratives to non-scientists about the oldest story of humanity: how from light, life grows; shown is a still from the IMAX dome theater movie 'Birth of Planet Earth'. 142

fluence on charge carrier mobility. However, diffusion timescales typically remain beyond the reach of brute force all-atom MD simulations and are instead addressed by MD-based coarse-grained protocols such as atomic resolution Brownian Dynamics (ARBD). ^{172,173} The resulting charge gradient generated across the membrane as a consequence of the aforementioned charge migration processes drives the synthesis of ATP (tens of milliseconds) at the ATP synthase, ^{146,167} culminating the conversion of solar energy into stable chemical bonds for later use.

An integrative computational model for energy conversion in a photosynthetic domain, by necessity, needs to involve multiple mathematical formulations that overlap in-sequence, i.e., with the output of each formulation being used as an input to the formulation at the next scale. ^{141,145,146} Through such overlapping formulations, primary observables such the ATP production rate (Fig. 3H) can be computed as a function of external conditions such as light intensity. ¹⁴⁶ The structural and functional model constructed in this manner guides MD simulations, enabling inquiry of refinements to energy conversion dynamics. This includes studying the effects of salinity on charge carrier diffusion. ³¹ When integrated over a cell-scale model incorporating a network of hundreds of chromatophores (Fig. 3J), the ATP production rate allows the quantification of a performance metric for the entire photosynthetic cell as an energy conversion device. his metric is known as the return-on-investment time (Fig. 3H) defined as the time it takes for the cell (or a part thereof) to produce enough ATP to pay for its initial construction cost in ATP. When adjusted for base metabolism, the return-on-investment time thus computed predicts the light dependence of cell doubling times (Fig. 3K) of *R. sphaeroides* over a wide range of light intensities. ¹⁴¹

The integrative approach for the energy conversion modeling presented above is *modular*, meaning that the mathematical formulations of rate kinetics at each scale can be refined further by simulations of spatial detail (e.g., via MD) as computational resources become abundant. Future challenges to computational studies of photosynthesis will involve both an expansion of time and length scales –to the cell level and beyond– as well as the refinement of each modular step in greater detail through simulation.

Outlook

As computational resources become cheaper and more powerful as outlined in Fig. 1, it is tempting to imagine that in order to achieve an integration of scales for bioenergetic processes, all one needs is to simply... wait. Namely that, perhaps, if we wait long enough, computational power would soon reach a scale that binds together the disparate scales of energy conversion. Alas, there are two primary problems with such optimism. First, though computational resources are becoming more abundant, the individual operation speed is no longer increasing prominently, ¹⁷⁴ and, therefore, basic timesteps of integration—typically on the order of a femtosecond for all-atom MD^{175} or an order of magnitude faster for CG-MD 176 -and, therefore, the timescales accessible directly by simulation do not improve substantially. Thus, the wide range of timescales for energy conversion, up to 12 orders of magnitude from excitation transfer to ATP synthesis, 141,146 will remain out of reach of integration by brute force simulation alone. Second, sampling of rate-limiting steps, particularly combined with the aforementioned difficulty of simulating slower processes, requires novel statistical approaches that rely on more than increasing simulation volume alone. These two problems combined imply that the future outlook for integrative simulations of bionergetic processes will for the foreseeable future involve computational advances and analytical advances in equal measure.

In recent years, there has been surge of interest in the study of active matter, especially in the exploration of living or artificial systems that use self-propulsion mechanisms to navigate through a fluid. Particles capable of absorbing energy from an external source, such as a laser beam, and subsequently utilizing that energy to induce motion through the dissipation of thermal energy, serve as an example of active matter. ¹⁷⁷ Prominent examples of such objects include diffusiophoretic colloidal Janus particles in a water-lutidine composite, ¹⁷⁸ chemically active microstructures, ^{179,180} thermophoretic microswimmers, ¹⁸¹ and magnetically responsive particles, ¹⁸² among a plethora of others. ¹⁸³ Recently, such active particles have found applications in phtosynthetic biotechnology. ¹⁸⁴ Cell organelles coated with photosystem II complexes are powered by light shows propulsion accross the stomach of the bowl-shaped vesicles. The oxygen produced by the water-splitting reaction by plant

organelles in visible light and the photophoresis effect due to the transparent nature of the supramolecular assembly are the main driving forces for bio-nanomotors. From a theoretical physics perspective, active particles can be examples of inherently non-equilibrium systems. The associated non-equilibrium attributes, such as the absence of detailed balance, interrelate with unconventional forms of interactions. To study these systems, the utilization of coarse-grained models in order to reduce the enormous degrees of freedom is critically important. These models must also describe key attributes such as sustained motion and the interactions among particles and the surrounding solvent. One foundational model aptly suited for this purpose is the active Brownian particle. This model integrates features from both translational and rotational Brownian motion, complemented by the introduction of a self-propulsive force acting upon the particle's body, while disregarding hydrodynamic interactions.¹⁸⁵

Energy conversion in the chromatophore (Fig. 3) provides an exemplar of how combined computational and analytical advances can bridge the disparate time and length scales sufficiently to have predictive power for cell scale observables, such as the cell doubling time as a function of growth light intensity. 141 Similar efforts are underway for cyanobacterial 186,187 and plant granal 188 photosynthetic systems. Bolstered by the dawn of exascale supercomputers (example, Oak Ridge National Laboratory's Frontier) that can perform up to 10¹⁸ floating point operations per second, molecular modeling is pushing the boundaries of cellscale simulations. This new horizon of analytical and computational advances stands to broaden the range over which bioenergetic processes can be integrated. Such integration would eventually enable rational design and optimization of bioenergy solutions 189,190 as well as assist biomedical approaches to respiratory diseases. ¹⁹¹ Furthermore, energy access is known to correlate with economic, environmental, and social benefits to human life, ¹⁹² with biological systems surpassing comparable human technologies in efficiency at systemslevel. 141 A renewable energy future will, therefore, benefit from advances in integrative modeling where we are challenged to not simply explain the behavior of a single protein, a single organelle, a single subsystem, or a single cell, but to optimize efficiency across many scales and systems, including all the way to that of the humans interacting with them.

Acknowledgments

S.M. thanks the Science and Engineering Research Board (SERB), Department of Science and Technology, Government of India, New Delhi, India (File no.: CRG/2022/002761). A.S. was supported by a CAREER award from the NSF (MCB-1942763) and an RO1 grant from the NIH (GM095583). A.S. also acknowledges start-up grants from Arizona State University School of Molecular Sciences and Biodesign Institute's Center for Applied Structural Discovery. A. S., M. S., and A. P. acknowledge funding from the Division of Chemical Sciences, Geosciences, and Biosciences, Office of Basic Energy Sciences, of the U.S. Department of Energy through grants DE-SC0010575. Additionally, R.M., A.S. and M.S. would like to apreciate grant DE-SC0022956 for their support, also from the Department of Energy.

Table 1. Prominent simulations of molecular bioenergetic systems over the last two decades: A chronological overview.

Year, System, Size	Method (Software), Length	Discovery	Experimental verification
2002 , LH-II complex, 87 000 atoms 55	QM/MD (NAMD), ~ 1 ns	Constructed a polaron model that allowed for the calculation of room temperature absorbance spectra and circular dichroism of LHII, which revealed de-localization of B850 BChl ring over 5 pigments.	LHII complex CD and Abs spectra ¹⁹³
2004 , F ₀ -ATPase, 111714 atoms ²¹	MD (NAMD) and mathematical modeling, 10 ns	Combining all-atom MD simulation and mathematical modeling to study how torque is generated in F_0 .	Heteronuclear single quantum coherence spectroscopy (HSQC) spectroscopy ¹⁹⁴
2004 , cyt. c oxidase aa3 type, $\sim 13000 \text{ atoms}^{195}$	GRID - MD, 1.125 ns	Providing insights into proton pumping by describing the hydrogen-bonded network and identifying key water molecule sites.	FTIR^{196}
2005 , Photosynthetic integral proteins and mobile carriers, † 96	m MC	Observed organizational effects among non-interacting particles that could be significant in reducing binding site obstructions.	N/A
2005 , POPC bilayer with Beta Carotenes, ~ 15000 atoms 197	MD (AMBER), 4 ns	Beta carotenes induce ordering effect on both chains of POPC	NMR and $EPR^{198,199}$
2006 , PS II, 236161 atoms 200	QM/MM (NAMD), 8ns	Calculated absorbance spectra, assigned PSII chlorophyll/Pheo site energies, and investigated the influence of thermal dynamic fluctuations on quantum efficieny.	Site directed mutagenesis and Spectroscopy 201,202
2010 , cyt. c - bc_1 complex, 275000 atoms 203	MD (NAMD), sub-nanosecond (150 ps)	The first MD simulation on the cyt c-bc ₁ complex interaction. Identified important salt bridges and hydrogen bonds between key residues at the interface.	X-Ray crystallography 204,205

2011 , Purple bacterial RC, $\sim 47000 \text{ atoms}^{69}$	SMD (GROMACS), $\sim 10 \text{ ns}$	Provided evidence for a larger Dissociation barrier for SQ^- compared to neutral Q in Q_A site of RC in contrast to their similar thermodynamic affinities.	Double-flash kinetic analysis ²⁰⁶
2013 , PS II, 1M atoms ⁸⁷	MD (AMBER), 10 ns	Proposed potential and relevant pathways of water movement in and out of PSII complex based on rms fluctuation analysis.	X-Ray crystallography ²⁰⁷
2013 , PS II and LHCII particles in stacked grana membranes, ‡ 208	MC	Formation of PSII arrays as evidence for co-existence of crystalline and fluid phases in thylakoid grana.	Electron Microscopy and Fluorescence induction ^{209,210}
2013 , Complex III and IV in POPC-CL membrane, 70000 beads ²¹¹	Course Grain (GROMACS/MARTINI), 490 μs	Identification of the favored interfaces of CLs on the respiratory chain complex III (cyt. bc_1).	CryoEM / EM 212
2014 , PS I in detergent belt, ~ 1 M atoms ²¹³	MD (NAMD), 40 or 200 ns	Lipid molecules play a role in stabilizing the PS1 trimer, some lipids are crucial for PsaL-mediated trimer stability.	X-Ray crystallography of integral membrane proteins ^{214,215}
2014 , PS II RC, 580000 atoms ²⁹	QM/MM (GROMACS), 30ns	Investigating how protein dynamics affect pigment site energies, influencing the preference for excitation pathways in the RC.	X-ray crystallography, transient absorption and 2D electronic spectroscopy ^{207,216,217}
2014 , Complex I, \sim 212000 atoms ²¹⁸	$850~\mathrm{ns}~\mathrm{MD}$ (NAMD) and $25~\mathrm{ps}$ QM/MM	Proposed that transient water chains create efficient paths for proton transfer, providing insights into long-range energy conversion in redox-driven proton-pumps.	$ m FTIR^{219}$
2015 , LHCII monomer, 100 K atoms ²²⁰	MD (GROMACS), 1 μs	Excitonic coupling strengths may be regulated and correlated to structural features such as N-terminus conformational disorder and Neoxanthin bending.	EPR, X-ray Crystallography ^{221,222}

2015 , PbRC, 94421 atoms ⁵⁰	MD (Anton), 11 μs	Proposed different wetting situation as the reason for unidirectionality of charge transfer between two quinone cofactors.	Spectroscopic data, The construction of a simple electronic device, a rectifier. Use of a single organic molecule ²²³
2015 , Complex I, ~ 810000 and 870000 atoms ²²⁴	MD (NAMD), QM/MM (QChem), $1.5~\mu\mathrm{s}$	Suggested that a distinctive interplay of electrostatic and conformational changes trigger proton pumping in complex I.	Electrochemistry experiments (redox activity measurement) ²²⁵
2015 , Plant and Cyanobacterial thylakoid membranes~130 K atoms ²²⁶	CG(GROMACS), 10 μs	Only nanoscale heterogeneities were detected in thylakoid membranes the cyanobacterial version of which, were shown to be thicker and less fluid than those of plants owing to high proportion of saturated tails.	$\mathrm{N/A}$
2016 , Purple bacterial cyt. c oxidase A1 type, † 227	CpHMD (GROMACS), 20ns (packing lipids) and 60 ns CpHMD	Conformational changes in specific Arginine residues may modulate protonation state of heme propionate residues that may be implicated in proton pumping.	$\mathrm{N/A}$
2016 , complex 1, 101440 atoms 228	QM/MD (MD (NAMD) and QM calculations based on perturbed matrix method), 250 ns	Developed an approach of energy gap usage for the estimation of the electron transfer rate by adding the polarizability effect.	Stark effect spectroscopy ²²⁹
2016 , Photosynthetic cyt. c_2 - bc_1 redox complex, 0.5 M atoms 127	MD/SMD and rigid body docking (NAMD), 200 ns (150ns MD and 50ns SMD)	Proposed mechanisms for the reversible binding interactions that mediate efficient electron transfer between cyt c2 and bc1 complex including the formation of a lysine molecular switch.	X-ray crystallography, Voltammetry ²³⁰
2017 , PS II, $^{\ddagger 88}$	CG (GROMACS), 60 μs	Differences exist in orientation between membrane-embedded PSII oligomeric states and in the mobility of photosynthetic cofactors depending on their location and type.	X-Ray Crystallography (B-factors) ²⁰⁷

2017 , phosphoglycerate mutase 1, \sim 29000 atoms* ²³¹	MD (Amber) and docking (Autodock), 200 ns	Proposed how phosphorylation at tyrosine 26 enhances the binding of phosphoglycerate mutase 1 (PGAM1) to its substrates.	N/A
2017 , V1-ATPase, 4.9 M atoms* 10	enhanced sampling and free energy methods, MD (NAMD), 65 $\mu \mathrm{s}$	Energy is harnessed at the subunit interfaces of the rotor ring whose central stalk exhibits mechanical properties suitable for rotation kinetics and the observed millisecond timescale.	X-ray crystallography ²³²
2018 , Purple bacterial LH2 and LH3 pigment proteins, ~ 1600000 atoms 233	MD and QM/MM (NAMD), 10ns (LH2) and 20ns (LH3)	Faster excitation trasfer within and between B820 and B800 rings in LH3 compared to LH2 rings.	N/A
2019 , Purple Bacterial Chromatophore, 136 M atoms ³¹	MD, QM, BD, CG (NAMD), 0.5 $\mu \mathrm{s}$	Proteins influence membrane curvature affecting light absorption, while the dynamics of soluble carriers play a role in ATP production's energetic output.	AFM, Cryo-EM, Spectroscopy 145,234,235
2020, Complex I, 1 M atoms ²⁰	MD (N/A) and free-energy calculations, 9.4 μs	Redox switches within complex I, allosterically couple the dynamics of the quinone binding pocket to the site of NADH reduction.	EPR^{236}
2022 , Hexokinase 2 with different ligands*, ^{‡ 237}	Docking (instaDock) and MD (GROMACS), 100 ns	HK2 readily forms stable protein-ligand complexes with both EGCG and quercitrin, maintaining stability throughout the entire simulation trajectory.	$\mathrm{N/A}$
2022 , V1-ATPase, 300 K atoms 75	MD (NAMD) and metadynamics calculation, 6.7 μs	Multiple intermediates along rotatory catalysis pathway of V1-ATPase.	Single molecule rotation assays ^{238,239}
2023 , F1-ATPase, 150 K atoms ⁷⁶	MD (GROMACS) and Bias exchange umbrella sampling, 4 μs	Nondissipative and kinetically fast progression of the motor in the synthesis direction requires a concerted conformational change.	N/A

^{*} Entries with this indicator are simulated without any membrane. [‡] Atom number not reported for entries with this indicator. Abbreviations: CL: cardiolipin; CD: circular dichroism; EGCG: epigallocatechin gallate; POPC: phosphatidylcholine; SQ: semiquinone.

References

- (1) Lavergne, J.; Joliot, P. Dissipation in bioenergetic electron transfer chains. *Photosynthesis research* **1996**, 48, 127–138.
- (2) Camargo, C. Physics makes rules, evolution rolls the dice. Science 2018, 361, 236–236.
- (3) Wilkinson, D. J. Stochastic modelling for quantitative description of heterogeneous biological systems.

 Nature Reviews Genetics 2009, 10, 122–133.
- (4) Goss, P. J.; Peccoud, J. Quantitative modeling of stochastic systems in molecular biology by using stochastic Petri nets. *Proceedings of the National Academy of Sciences* **1998**, *95*, 6750–6755.
- (5) Wang, Y.; Han, N.; Li, X.; Yu, S.; Xing, L. Artificial light-harvesting systems and their applications in photocatalysis and cell labeling. *ChemPhysMater* **2022**, *1*, 281–293.
- (6) Marullo, R.; Werner, E.; Degtyareva, N.; Moore, B.; Altavilla, G.; Ramalingam, S. S.; Doetsch, P. W. Cisplatin induces a mitochondrial-ROS response that contributes to cytotoxicity depending on mitochondrial redox status and bioenergetic functions. *PloS one* **2013**, *8*, e81162.
- (7) Teoh, S. T.; Lunt, S. Y. Metabolism in cancer metastasis: bioenergetics, biosynthesis, and beyond. Wiley Interdisciplinary Reviews: Systems Biology and Medicine 2018, 10, e1406.
- (8) Strope, T. A.; Birky, C. J.; Wilkins, H. M. The role of bioenergetics in neurodegeneration. *International Journal of Molecular Sciences* **2022**, *23*, 9212.
- (9) Mitchell, P. Coupling of phosphorylation to electron and hydrogen transfer by a chemi-osmotic type of mechanism. *Nature* **1961**, *191*, 144–148.
- (10) Singharoy, A.; Chipot, C.; Moradi, M.; Schulten, K. Chemomechanical Coupling in Hexameric Protein-Protein Interfaces Harnesses Energy within V-Type ATPases. J. Am. Chem. Soc. 2017, 139, 293–310.
- (11) Alberts, B.; Johnson, A.; Lewis, J.; Raff, M.; Roberts, K.; Walter, P. Molecular Biology of the Cell. 4th edition; Garland Science, 2002.
- (12) Arnold, S. The power of life—cytochrome c oxidase takes center stage in metabolic control, cell signalling and survival. *Mitochondrion* **2012**, *12*, 46–56.
- (13) Walker, J. E. ATP synthesis by rotary catalysis (Nobel Lecture). Angewandte Chemie International Edition 1998, 37, 2308–2319.

- (14) Liberti, M. V.; Locasale, J. W. The Warburg effect: how does it benefit cancer cells? *Trends in biochemical sciences* **2016**, *41*, 211–218.
- (15) Nogales, J.; Gudmundsson, S.; Knight, E. M.; Palsson, B. O.; Thiele, I. Detailing the optimality of photosynthesis in cyanobacteria through systems biology analysis. *Proceedings of the National Academy of Sciences* **2012**, *109*, 2678–2683.
- (16) Saks, V. Molecular System Bioenergetics—New Aspects of Metabolic Research. *International Journal of Molecular Sciences* **2009**, *10*, 3655–3657.
- (17) Liguori, N.; Croce, R.; Marrink, S. J.; Thallmair, S. Molecular dynamics simulations in photosynthesis. *Photosynthesis research* **2020**, *144*, 273–295.
- (18) Janosi, L.; Kosztin, I.; Damjanović, A. Theoretical prediction of spectral and optical properties of bacteriochlorophylls in thermally disordered LH2 antenna complexes. The Journal of chemical physics 2006, 125, 014903.
- (19) Van Eerden, F. J.; Melo, M. N.; Frederix, P. W.; Periole, X.; Marrink, S. J. Exchange pathways of plastoquinone and plastoquinol in the photosystem II complex. *Nature communications* **2017**, *8*, 15214.
- (20) Gupta, C.; Khaniya, U.; Chan, C. K.; Dehez, F.; Shekhar, M.; Gunner, M.; Sazanov, L.; Chipot, C.; Singharoy, A. Charge transfer and chemo-mechanical coupling in respiratory complex I. *Journal of the American Chemical Society* **2020**, *142*, 9220–9230.
- (21) Aksimentiev, A.; Balabin, I. A.; Fillingame, R. H.; Schulten, K. Insights into the Molecular Mechanism of Rotation in the Fo sector of ATP Synthase. *Biophys. J.* **2004**, *86*, 1332–1344.
- (22) Karplus, M.; McCammon, J. A. Molecular dynamics simulations of biomolecules. *Nat. Struct. Biol.* **2002**, 265, 654–652.
- (23) Dror, R. O.; Dirks, R. M.; Grossman, J.; Xu, H.; Shaw, D. E. Biomolecular simulation: a computational microscope for molecular biology. *Annual review of biophysics* **2012**, *41*, 429–452.
- (24) Jones, D.; Allen, J. E.; Yang, Y.; Drew Bennett, W. F.; Gokhale, M.; Moshiri, N.; Rosing, T. S. Accelerators for classical molecular dynamics simulations of biomolecules. *Journal of chemical theory and computation* **2022**, *18*, 4047–4069.
- (25) Stone, J. E.; Phillips, J. C.; Freddolino, P. L.; Hardy, D. J.; Trabuco, L. G.; Schulten, K. Accelerating molecular modeling applications with graphics processors. *Journal of computational chemistry* 2007, 28, 2618–2640.

- (26) Jász, Á.; Rák, Á.; Ladjánszki, I.; Cserey, G. Classical molecular dynamics on graphics processing unit architectures. Wiley Interdisciplinary Reviews: Computational Molecular Science 2020, 10, e1444.
- (27) Mei, C.; Sun, Y.; Zheng, G.; Bohm, E. J.; Kale, L. V.; Phillips, J. C.; Harrison, C. Enabling and scaling biomolecular simulations of 100 million atoms on petascale machines with a multicore-optimized message-driven runtime. Proceedings of 2011 International Conference for High Performance Computing, Networking, Storage and Analysis. 2011; pp 1–11.
- (28) Shaw, D. E.; Grossman, J.; Bank, J. A.; Batson, B.; Butts, J. A.; Chao, J. C.; Deneroff, M. M.; Dror, R. O.; Even, A.; Fenton, C. H. et al. Anton 2: raising the bar for performance and programmability in a special-purpose molecular dynamics supercomputer. SC'14: Proceedings of the International Conference for High Performance Computing, Networking, Storage and Analysis. 2014; pp 41–53.
- (29) Zhang, L.; Silva, D.-A.; Zhang, H.; Yue, A.; Yan, Y.; Huang, X. Dynamic protein conformations preferentially drive energy transfer along the active chain of the photosystem II reaction centre. *Nature Communications* **2014**, *5*, 4170.
- (30) Kulik, N.; Kutỳ, M.; Řeha, D. The study of conformational changes in photosystem II during a charge separation. *Journal of Molecular Modeling* **2020**, *26*, 1–13.
- (31) Singharoy, A.; Maffeo, C.; Delgado-Magnero, K. H.; Swainsbury, D. J.; Sener, M.; Kleinekathöfer, U.; Vant, J. W.; Nguyen, J.; Hitchcock, A.; Isralewitz, B. et al. Atoms to phenotypes: molecular design principles of cellular energy metabolism. Cell 2019, 179, 1098–1111.
- (32) Jung, J.; Kobayashi, C.; Kasahara, K.; Tan, C.; Kuroda, A.; Minami, K.; Ishiduki, S.; Nishiki, T.; Inoue, H.; Ishikawa, Y. et al. New parallel computing algorithm of molecular dynamics for extremely huge scale biological systems. *Journal of computational chemistry* **2021**, *42*, 231–241.
- (33) Zuckerman, D. M. Equilibrium sampling in biomolecular simulations. *Annual review of biophysics* **2011**, 40, 41–62.
- (34) Cisneros, G. A.; Karttunen, M.; Ren, P.; Sagui, C. Classical electrostatics for biomolecular simulations. Chemical reviews 2014, 114, 779–814.
- (35) Jing, Z.; Liu, C.; Cheng, S. Y.; Qi, R.; Walker, B. D.; Piquemal, J.-P.; Ren, P. Polarizable force fields for biomolecular simulations: Recent advances and applications. *Annual Review of biophysics* **2019**, *48*, 371–394.

- (36) Adam, S.; Knapp-Mohammady, M.; Yi, J.; Bondar, A.-N. Revised CHARMM force field parameters for iron-containing cofactors of photosystem II. *Journal of Computational Chemistry* **2018**, *39*, 7–20.
- (37) Marx, D.; Hutter, J. Ab initio molecular dynamics: basic theory and advanced methods; Cambridge University Press, 2009.
- (38) Car, R.; Parrinello, M. Unified approach for molecular dynamics and density-functional theory. *Physical review letters* **1985**, *55*, 2471.
- (39) Christensen, A. S.; Kubar, T.; Cui, Q.; Elstner, M. Semiempirical quantum mechanical methods for noncovalent interactions for chemical and biochemical applications. *Chemical Reviews* 2016, 116, 5301– 5337.
- (40) Brunk, E.; Rothlisberger, U. Mixed quantum mechanical/molecular mechanical molecular dynamics simulations of biological systems in ground and electronically excited states. *Chemical reviews* **2015**, *115*, 6217–6263.
- (41) Vitillo, J. G.; Cramer, C. J.; Gagliardi, L. Multireference methods are realistic and useful tools for modeling catalysis. *Israel Journal of Chemistry* **2022**, *62*, e202100136.
- (42) Dreuw, A.; Head-Gordon, M. Single-reference ab initio methods for the calculation of excited states of large molecules. *Chemical reviews* **2005**, *105*, 4009–4037.
- (43) Sherrill, C. D.; Schaefer III, H. F. Advances in quantum chemistry; Elsevier, 1999; Vol. 34; pp 143–269.
- (44) Huix-Rotllant, M.; Ferré, N.; Barbatti, M. Time-dependent density functional theory. Quantum Chemistry and Dynamics of Excited States: Methods and Applications 2020, 13–46.
- (45) Runge, E.; Gross, E. K. Density-functional theory for time-dependent systems. *Physical review letters* 1984, 52, 997.
- (46) Grimme, S.; Waletzke, M. A combination of Kohn–Sham density functional theory and multi-reference configuration interaction methods. *The Journal of chemical physics* **1999**, *111*, 5645–5655.
- (47) Lyskov, I.; Kleinschmidt, M.; Marian, C. M. Redesign of the DFT/MRCI Hamiltonian. *The Journal of chemical physics* **2016**, *144*, 034104.
- (48) Toporik, H.; Li, J.; Williams, D.; Chiu, P.-L.; Mazor, Y. The structure of the stress-induced photosystem I–IsiA antenna supercomplex. *Nature Structural & Molecular Biology* **2019**, *26*, 443–449.

- (49) Zhang, L.; Silva, D.-A.; Yan, Y.; Huang, X. Force field development for cofactors in the photosystem II.

 Journal of computational chemistry 2012, 33, 1969–1980.
- (50) Martin, D. R.; Matyushov, D. V. Photosynthetic diode: Electron transport rectification by wetting the quinone cofactor. *Physical Chemistry Chemical Physics* **2015**, *17*, 22523–22528.
- (51) Grimme, S.; Antony, J.; Ehrlich, S.; Krieg, H. A consistent and accurate ab initio parametrization of density functional dispersion correction (DFT-D) for the 94 elements H-Pu. *The Journal of chemical physics* **2010**, *132*, 154104.
- (52) Ambrosetti, A.; Reilly, A. M.; DiStasio, R. A.; Tkatchenko, A. Long-range correlation energy calculated from coupled atomic response functions. *The Journal of chemical physics* **2014**, *140*, 18A508.
- (53) Warshel, A.; Levitt, M. Theoretical studies of enzymic reactions: dielectric, electrostatic and steric stabilization of the carbonium ion in the reaction of lysozyme. *Journal of molecular biology* **1976**, 103, 227–249.
- (54) Meier, K.; Thiel, W.; van Gunsteren, W. F. On the effect of a variation of the force field, spatial boundary condition and size of the QM region in QM/MM MD simulations. *Journal of computational chemistry* **2012**, *33*, 363–378.
- (55) Damjanović, A.; Kosztin, I.; Kleinekathoefer, U.; Schulten, K. Excitons in a Photosynthetic Light-Harvesting System: A Combined Molecular Dynamics, Quantum Chemistry and Polaron Model Study. *Phys. Rev. E* **2002**, *65*, 031919, (24 pages).
- (56) Maity, S.; Daskalakis, V.; Elstner, M.; Kleinekathöfer, U. Multiscale QM/MM molecular dynamics simulations of the trimeric major light-harvesting complex II. Physical Chemistry Chemical Physics 2021, 23, 7407–7417.
- (57) Lischka, H.; Nachtigallova, D.; Aquino, A. J.; Szalay, P. G.; Plasser, F.; Machado, F. B.; Barbatti, M. Multireference approaches for excited states of molecules. *Chemical reviews* **2018**, *118*, 7293–7361.
- (58) Werner, H.-J.; Knowles, P. J. An efficient internally contracted multiconfiguration—reference configuration interaction method. *The Journal of chemical physics* **1988**, *89*, 5803–5814.
- (59) Goll, E.; Leininger, T.; Manby, F. R.; Mitrushchenkov, A.; Werner, H.-J.; Stoll, H. Local and density fitting approximations within the short-range/long-range hybrid scheme: application to large non-bonded complexes. *Physical Chemistry Chemical Physics* **2008**, *10*, 3353–3357.

- (60) Ferré, N.; Guihéry, N.; Malrieu, J.-P. Spin decontamination of broken-symmetry density functional theory calculations: deeper insight and new formulations. *Physical Chemistry Chemical Physics* 2015, 17, 14375– 14382.
- (61) Perdew, J. P.; Tao, J.; Staroverov, V. N.; Scuseria, G. E. Meta-generalized gradient approximation: Explanation of a realistic nonempirical density functional. The Journal of chemical physics 2004, 120, 6898–6911.
- (62) Blachly, P. G.; Sandala, G. M.; Giammona, D. A.; Liu, T.; Bashford, D.; McCammon, J. A.; Noodleman, L. Use of broken-symmetry density functional theory to characterize the IspH oxidized state: Implications for IspH mechanism and inhibition. *Journal of chemical theory and computation* 2014, 10, 3871–3884.
- (63) Bernardi, R. C.; Melo, M. C.; Schulten, K. Enhanced sampling techniques in molecular dynamics simulations of biological systems. *Biochimica et Biophysica Acta (BBA)-General Subjects* **2015**, *1850*, 872–877.
- (64) Dellago, C.; Bolhuis, P. G. Transition path sampling and other advanced simulation techniques for rare events. Advanced computer simulation approaches for soft matter sciences III 2009, 167–233.
- (65) Kästner, J. Umbrella sampling. Wiley Interdisciplinary Reviews: Computational Molecular Science 2011, 1, 932–942.
- (66) Izrailev, S.; Stepaniants, S.; Isralewitz, B.; Kosztin, D.; Lu, H.; Molnar, F.; Wriggers, W.; Schulten, K. Steered molecular dynamics. Computational Molecular Dynamics: Challenges, Methods, Ideas: Proceedings of the 2nd International Symposium on Algorithms for Macromolecular Modelling, Berlin, May 21–24, 1997. 1999; pp 39–65.
- (67) Mao, R.; Zhang, H.; Bie, L.; Liu, L.-N.; Gao, J. Million-atom molecular dynamics simulations reveal the interfacial interactions and assembly of plant PSII-LHCII supercomplex. RSC advances 2023, 13, 6699–6712.
- (68) Paddock, M.; Flores, M.; Isaacson, R.; Chang, C.; Abresch, E.; Okamura, M. ENDOR Spectroscopy Reveals Light Induced Movement of the H-Bond from Ser-L223 upon Forming the Semiquinone (QB-●) in Reaction Centers from Rhodobacter sphaeroide s. *Biochemistry* **2007**, *46*, 8234–8243.
- (69) Madeo, J.; Mihajlovic, M.; Lazaridis, T.; Gunner, M. R. Slow Dissociation of a Charged Ligand: Analysis of the Primary Quinone Q_A Site of Photosynthetic Bacterial Reaction Centers. J. Am. Chem. Soc. 2011, 133, 17375–17385.

- (70) Warnau, J.; Sharma, V.; Gamiz-Hernandez, A. P.; Di Luca, A.; Haapanen, O.; Vattulainen, I.; Wikström, M.; Hummer, G.; Kaila, V. R. Redox-coupled quinone dynamics in the respiratory complex I. *Proceedings of the National Academy of Sciences* **2018**, *115*, E8413–E8420.
- (71) Boubeta, F. M.; Contestín García, R. M.; Lorenzo, E. N.; Boechi, L.; Estrin, D.; Sued, M.; Arrar, M. Lessons learned about steered molecular dynamics simulations and free energy calculations. *Chemical biology & drug design* **2019**, *93*, 1129–1138.
- (72) Ozer, G.; Valeev, E. F.; Quirk, S.; Hernandez, R. Adaptive steered molecular dynamics of the long-distance unfolding of neuropeptide Y. *Journal of Chemical Theory and Computation* **2010**, *6*, 3026–3038.
- (73) Laio, A.; Parrinello, M. Escaping free-energy minima. *Proceedings of the national academy of sciences* **2002**, *99*, 12562–12566.
- (74) Barducci, A.; Bonomi, M.; Parrinello, M. Metadynamics. Wiley Interdisciplinary Reviews: Computational Molecular Science 2011, 1, 826–843.
- (75) Shekhar, M.; Gupta, C.; Suzuki, K.; Chan, C. K.; Murata, T.; Singharoy, A. Revealing a hidden intermediate of rotatory catalysis with X-ray crystallography and Molecular simulations. *ACS Central Science* **2022**, *8*, 915–925.
- (76) Badocha, M.; Wieczór, M.; Marciniak, A.; Kleist, C.; Grubmüller, H.; Czub, J. Molecular mechanism and energetics of coupling between substrate binding and product release in the F1-ATPase catalytic cycle.

 Proceedings of the National Academy of Sciences 2023, 120, e2215650120.
- (77) Wang, J.; Ishchenko, A.; Zhang, W.; Razavi, A.; Langley, D. A highly accurate metadynamics-based Dissociation Free Energy method to calculate protein–protein and protein–ligand binding potencies. *Scientific Reports* 2022, 12, 2024.
- (78) Patel, J. S.; Ytreberg, F. M. Fast calculation of protein–protein binding free energies using umbrella sampling with a coarse-grained model. *Journal of chemical theory and computation* **2018**, *14*, 991–997.
- (79) Fiorin, G.; Pastore, A.; Carloni, P.; Parrinello, M. Using metadynamics to understand the mechanism of calmodulin/target recognition at atomic detail. *Biophysical Journal* **2006**, *91*, 2768–2777.
- (80) Singharoy, A.; Teo, I.; McGreevy, R.; Stone, J. E.; Zhao, J.; Schulten, K. Molecular dynamics-based refinement and validation for sub-5 Å cryo-electron microscopy maps. *Elife* **2016**, *5*, e16105.

- (81) Shekhar, M.; Terashi, G.; Gupta, C.; Sarkar, D.; Debussche, G.; Sisco, N. J.; Nguyen, J.; Mondal, A.; Vant, J.; Fromme, P. et al. CryoFold: Determining protein structures and data-guided ensembles from cryo-EM density maps. *Matter* **2021**, *4*, 3195–3216.
- (82) Vant, J. W.; Sarkar, D.; Nguyen, J.; Baker, A. T.; Vermaas, J. V.; Singharoy, A. Exploring cryo-electron microscopy with molecular dynamics. *Biochemical Society Transactions* **2022**, *50*, 569–581.
- (83) Saunders, M. G.; Voth, G. A. Coarse-graining methods for computational biology. *Annual review of biophysics* **2013**, *42*, 73–93.
- (84) Noid, W. G. Perspective: Coarse-grained models for biomolecular systems. *The Journal of chemical physics* **2013**, *139*, 090901.
- (85) Izvekov, S.; Voth, G. A. A multiscale coarse-graining method for biomolecular systems. *The Journal of Physical Chemistry B* **2005**, *109*, 2469–2473.
- (86) Jumper, J. M.; Faruk, N. F.; Freed, K. F.; Sosnick, T. R. Trajectory-based training enables protein simulations with accurate folding and Boltzmann ensembles in cpu-hours. *PLoS computational biology* **2018**, *14*, e1006578.
- (87) Ogata, K.; Yuki, T.; Hatakeyama, M.; Uchida, W.; Nakamura, S. All-atom molecular dynamics simulation of photosystem II embedded in thylakoid membrane. *Journal of the American Chemical Society* **2013**, 135, 15670–15673.
- (88) Van Eerden, F. J.; Van Den Berg, T.; Frederix, P. W.; De Jong, D. H.; Periole, X.; Marrink, S. J. Molecular dynamics of photosystem II embedded in the thylakoid membrane. *The Journal of Physical Chemistry B* **2017**, *121*, 3237–3249.
- (89) Arnarez, C.; Marrink, S.; Periole, X. Identification of cardiolipin binding sites on cytochrome c oxidase at the entrance of proton channels. *Scientific reports* **2013**, *3*, 1263.
- (90) Ingólfsson, H. I.; Lopez, C. A.; Uusitalo, J. J.; de Jong, D. H.; Gopal, S. M.; Periole, X.; Marrink, S. J. The power of coarse graining in biomolecular simulations. Wiley Interdisciplinary Reviews: Computational Molecular Science 2014, 4, 225–248.
- (91) Debnath, A.; Wiegand, S.; Paulsen, H.; Kremer, K.; Peter, C. Derivation of coarse-grained simulation models of chlorophyll molecules in lipid bilayers for applications in light harvesting systems. *Physical Chemistry Chemical Physics* **2015**, *17*, 22054–22063.

- (92) Marrink, S. J.; Risselada, H. J.; Yefimov, S.; Tieleman, D. P.; De Vries, A. H. The MARTINI force field: coarse grained model for biomolecular simulations. *The journal of physical chemistry B* **2007**, *111*, 7812–7824.
- (93) De Jong, D. H.; Liguori, N.; Van Den Berg, T.; Arnarez, C.; Periole, X.; Marrink, S. J. Atomistic and coarse grain topologies for the cofactors associated with the photosystem II core complex. *The Journal of Physical Chemistry B* **2015**, *119*, 7791–7803.
- (94) Thallmair, S.; Vainikka, P. A.; Marrink, S. J. Lipid fingerprints and cofactor dynamics of light-harvesting complex II in different membranes. *Biophysical journal* **2019**, *116*, 1446–1455.
- (95) Tremmel, I.; Kirchhoff, H.; Weis, E.; Farquhar, G. Dependence of plastoquinol diffusion on the shape, size, and density of integral thylakoid proteins. *Biochimica et Biophysica Acta (BBA)-Bioenergetics* **2003**, 1607, 97–109.
- (96) Tremmel, I.; Weis, E.; Farquhar, G. The influence of protein-protein interactions on the organization of proteins within thylakoid membranes. *Biophysical journal* **2005**, 88, 2650–2660.
- (97) Song, Y.; Mao, J.; Gunner, M. R. MCCE2: improving protein pKa calculations with extensive side chain rotamer sampling. *Journal of computational chemistry* **2009**, *30*, 2231–2247.
- (98) Cabeza de Vaca, I.; Qian, Y.; Vilseck, J. Z.; Tirado-Rives, J.; Jorgensen, W. L. Enhanced Monte Carlo methods for modeling proteins including computation of absolute free energies of binding. *Journal of chemical theory and computation* **2018**, *14*, 3279–3288.
- (99) Wood, W. H.; Johnson, M. P. Modeling the role of LHCII-LHCII, PSII-LHCII, and PSI-LHCII interactions in state transitions. *Biophysical Journal* **2020**, *119*, 287–299.
- (100) Zhang, Z.; Ehmann, U.; Zacharias, M. Monte Carlo replica-exchange based ensemble docking of protein conformations. *Proteins: Structure, Function, and Bioinformatics* **2017**, *85*, 924–937.
- (101) Earl, D. J.; Deem, M. W. Parallel tempering: Theory, applications, and new perspectives. *Physical Chemistry Chemical Physics* **2005**, *7*, 3910–3916.
- (102) Cole, D. J.; Tirado-Rives, J.; Jorgensen, W. L. Enhanced Monte Carlo sampling through replica exchange with solute tempering. *Journal of chemical theory and computation* **2014**, *10*, 565–571.
- (103) Liu, P.; Kim, B.; Friesner, R. A.; Berne, B. J. Replica exchange with solute tempering: A method for sampling biological systems in explicit water. *Proceedings of the National Academy of Sciences* 2005, 102, 13749–13754.

- (104) Lüchow, A. Quantum monte carlo methods. Wiley Interdisciplinary Reviews: Computational Molecular Science 2011, 1, 388–402.
- (105) Scemama, A.; Caffarel, M.; Oseret, E.; Jalby, W. Quantum Monte Carlo for large chemical systems: Implementing efficient strategies for petascale platforms and beyond. *Journal of computational chemistry* **2013**, *34*, 938–951.
- (106) Austin, B. M.; Zubarev, D. Y.; Lester Jr, W. A. Quantum Monte Carlo and related approaches. *Chemical reviews* **2012**, *112*, 263–288.
- (107) Aspuru-Guzik, A.; Lester Jr, W. A. Quantum Monte Carlo methods for the solution of the Schrödinger equation for molecular systems. *Handbook of Numerical Analysis* **2003**, *10*, 485–535.
- (108) Chen, W.; Morrow, B. H.; Shi, C.; Shen, J. K. Recent development and application of constant pH molecular dynamics. *Molecular simulation* **2014**, *40*, 830–838.
- (109) Itoh, S. G.; Damjanović, A.; Brooks, B. R. pH replica-exchange method based on discrete protonation states. *Proteins: Structure, Function, and Bioinformatics* **2011**, *79*, 3420–3436.
- (110) Meng, Y.; Roitberg, A. E. Constant pH replica exchange molecular dynamics in biomolecules using a discrete protonation model. *Journal of chemical theory and computation* **2010**, *6*, 1401–1412.
- (111) de Oliveira, V. M.; Liu, R.; Shen, J. Constant ph molecular dynamics simulations: current status and recent applications. *Current opinion in structural biology* **2022**, *77*, 102498.
- (112) Liguori, N.; Campos, S. R.; Baptista, A. M.; Croce, R. Molecular anatomy of plant photoprotective switches: the sensitivity of PsbS to the environment, residue by residue. *The journal of physical chemistry letters* **2019**, *10*, 1737–1742.
- (113) Pedraza-González, L.; Cignoni, E.; D'Ascenzi, J.; Cupellini, L.; Mennucci, B. How the pH controls photoprotection in the light-harvesting complex of mosses. *Journal of the American Chemical Society* **2023**, 145, 7482–7494.
- (114) Khaniya, U.; Mao, J.; Wei, R. J.; Gunner, M. Characterizing protein protonation microstates using Monte Carlo sampling. *The Journal of Physical Chemistry B* **2022**, *126*, 2476–2485.
- (115) Northrup, S. H.; Boles, J. O.; Reynolds, J. C. Electrostatic effects in the Brownian dynamics of association and orientation of heme proteins. *Journal of Physical Chemistry* **1987**, *91*, 5991–5998.

- (116) Northrup, S. H.; Luton, J. A.; Boles, J. O.; Reynolds, J. C. Brownian dynamics simulation of protein association. *Journal of Computer-Aided Molecular Design* 1988, 1, 291–311.
- (117) Gabdoulline, R. R.; Wade, R. C. Protein-protein association: investigation of factors influencing association rates by Brownian dynamics simulations. *Journal of molecular biology* **2001**, *306*, 1139–1155.
- (118) Solano, C. J. F. The BROMOCEA Code: An Improved Grand Canonical Monte Carlo/Brownian Dynamics Algorithm Including Explicit Atoms. *Biophysical Journal* **2016**, *110*, 328a.
- (119) Solano, C. J.; Prajapati, J. D.; Pothula, K. R.; Kleinekathöfer, U. Brownian dynamics approach including explicit atoms for studying ion permeation and substrate translocation across nanopores. *Journal of chemical theory and computation* **2018**, *14*, 6701–6713.
- (120) Kosztin, I.; Schulten, K. Biophysical techniques in photosynthesis; Springer, 2008; pp 445–464.
- (121) Sener, M.; Strümpfer, J.; Hsin, J.; Chandler, D.; Scheuring, S.; Hunter, C. N.; Schulten, K. Förster energy transfer theory as reflected in the structures of photosynthetic light harvesting systems. *Chem. Phys. Chem.* **2011**, *12*, 518–531.
- (122) Linnanto, J.; Korppi-Tommola, J. Quantum chemical simulation of excited states of chlorophylls, bacteriochlorophylls and their complexes. *Physical Chemistry Chemical Physics* **2006**, *8*, 663–687.
- (123) Ferretti, M.; Hendrikx, R.; Romero, E.; Southall, J.; Cogdell, R. J.; Novoderezhkin, V. I.; Scholes, G. D.; Van Grondelle, R. Dark states in the light-harvesting complex 2 revealed by two-dimensional electronic spectroscopy. *Scientific reports* **2016**, *6*, 20834.
- (124) Van Eerden, F. J.; Melo, M. N.; Frederix, P. W.; Marrink, S. J. Prediction of thylakoid lipid binding sites on photosystem II. *Biophysical journal* **2017**, *113*, 2669–2681.
- (125) Cignoni, E.; Slama, V.; Cupellini, L.; Mennucci, B. The atomistic modeling of light-harvesting complexes from the physical models to the computational protocol. *The Journal of Chemical Physics* **2022**, *156*, 120901.
- (126) Tamura, H.; Saito, K.; Ishikita, H. The origin of unidirectional charge separation in photosynthetic reaction centers: nonadiabatic quantum dynamics of exciton and charge in pigment–protein complexes.

 Chemical science 2021, 12, 8131–8140.
- (127) Singharoy, A.; Barragan, A. M.; Thangapandian, S.; Tajkhorshid, E.; Schulten, K. Binding site recognition and docking dynamics of a single electron transport protein: Cytochrome c 2. *Journal of the American Chemical Society* **2016**, *138*, 12077–12089.

- (128) Pogorelov, T. V.; Autenrieth, F.; Roberts, E.; Luthey-Schulten, Z. A. Cytochrome c2 exit strategy: dissociation studies and evolutionary implications. *The Journal of Physical Chemistry B* **2007**, *111*, 618–634.
- (129) Pietras, R.; Sarewicz, M.; Osyczka, A. Molecular Organization of Cytochrome c 2 near the Binding Domain of Cytochrome bc 1 Studied by Electron Spin–Lattice Relaxation Enhancement. *The Journal of Physical Chemistry B* **2014**, *118*, 6634–6643.
- (130) Cramer, W. A.; Hasan, S. S.; Yamashita, E. The Q cycle of cytochrome bc complexes: a structure perspective. *Biochimica et Biophysica Acta (BBA)-Bioenergetics* **2011**, *1807*, 788–802.
- (131) Barragan, A. M.; Crofts, A. R.; Schulten, K.; Solov'yov, I. A. Identification of ubiquinol binding motifs at the Q o-site of the cytochrome bc 1 complex. *The Journal of Physical Chemistry B* **2015**, *119*, 433–447.
- (132) Barragan, A. M.; Schulten, K.; Solov'yov, I. A. Mechanism of the primary charge transfer reaction in the cytochrome bc 1 complex. *The Journal of Physical Chemistry B* **2016**, *120*, 11369–11380.
- (133) Barragan, A. M.; Soudackov, A. V.; Luthey-Schulten, Z.; Hammes-Schiffer, S.; Schulten, K.; Solov'yov, I. A. Theoretical description of the primary proton-coupled electron transfer reaction in the cytochrome bc 1 complex. *Journal of the American Chemical Society* **2021**, *143*, 715–723.
- (134) Singharoy, A.; Chipot, C.; Ekimoto, T.; Suzuki, K.; Ikeguchi, M.; Yamato, I.; Murata, T. Rotational mechanism model of the bacterial V1 motor based on structural and computational analyses. *Frontiers in Physiology* **2019**, *10*, 46.
- (135) Roh, S.-H.; Shekhar, M.; Pintilie, G.; Chipot, C.; Wilkens, S.; Singharoy, A.; Chiu, W. Cryo-EM and MD infer water-mediated proton transport and autoinhibition mechanisms of Vo complex. *Science Advances* **2020**, *6*, eabb9605.
- (136) Anandakrishnan, R.; Zhang, Z.; Donovan-Maiye, R.; Zuckerman, D. M. Biophysical comparison of ATP synthesis mechanisms shows a kinetic advantage for the rotary process. *Proceedings of the National Academy of Sciences* **2016**, *113*, 11220–11225.
- (137) Czub, J.; Grubmüller, H. Rotation Triggers Nucleotide-Independent Conformational Transition of the Empty β Subunit of F1-ATPase. Journal of the American Chemical Society **2014**, 136, 6960–6968.
- (138) Böckmann, R. A.; Grubmüller, H. Nanoseconds molecular dynamics simulation of primary mechanical energy transfer steps in F1-ATP synthase. *Nature structural biology* **2002**, *9*, 198–202.

- (139) Czub, J.; Grubmüller, H. Torsional elasticity and energetics of F1-ATPase. *Proceedings of the National Academy of Sciences* **2011**, *108*, 7408–7413.
- (140) Mukherjee, S.; Warshel, A. The FOF 1 ATP synthase: from atomistic three-dimensional structure to the rotary-chemical function. *Photosynthesis research* **2017**, *134*, 1–15.
- (141) Hitchcock, A.; Hunter, C. N.; Sener, M. Determination of cell doubling times from the return-on-investment time of photosynthetic vesicles based on atomic detail structural models. J. Phys. Chem. B 2017, 121, 3787–3797.
- (142) Sener, M.; Levy, S.; Stone, J. E.; Christensen, A.; Isralewitz, B.; Patterson, R.; Borkiewicz, K.; Carpenter, J.; Hunter, C. N.; Luthey-Schulten, Z. et al. Multiscale modeling and cinematic visualization of photosynthetic energy conversion processes from electronic to cell scales. *Parallel computing* **2021**, *102*, 102698.
- (143) Sener, M. K.; Olsen, J. D.; Hunter, C. N.; Schulten, K. Atomic level structural and functional model of a bacterial photosynthetic membrane vesicle. *Proc. Natl. Acad. Sci. USA* **2007**, *104*, 15723–15728.
- (144) Sener, M.; Strumpfer, J.; Timney, J. A.; Freiberg, A.; Hunter, C. N.; Schulten, K. Photosynthetic Vesicle Architecture and Constraints on Efficient Energy Harvesting. *Biophys. J.* **2010**, *99*, 67–75.
- (145) Cartron, M. L.; Olsen, J. D.; Sener, M.; Jackson, P. J.; Brindley, A. A.; Qian, P.; Dickman, M. J.; Leggett, G. J.; Schulten, K.; Hunter, C. N. Integration of energy and electron transfer processes in the photosynthetic membrane of *Rhodobacter sphaeroides*. *Biochim. Biophys. Acta, Bioener.* 2014, 1837, 1769–1780.
- (146) Sener, M.; Strumpfer, J.; Singharoy, A.; Hunter, C. N.; Schulten, K. Overall energy conversion efficiency of a photosynthetic vesicle. *Elife* **2016**, *5*, e09541.
- (147) Bahatyrova, S.; Frese, R. N.; Siebert, C. A.; Olsen, J. D.; van der Werf, K. O.; van Grondelle, R.; Niederman, R. A.; Bullough, P. A.; Otto, C.; Hunter, C. N. The native architecture of a photosynthetic membrane. *Nature* **2004**, *430*, 1058–1062.
- (148) Olsen, J. D.; Tucker, J. D.; Timney, J. A.; Qian, P.; Vassilev, C.; Hunter, C. N. The organization of LH2 complexes in membranes from *Rhodobacter sphaeroides*. *J. Biol. Chem.* **2008**, *283*, 30772–30779.
- (149) Qian, P.; Hunter, C. N.; Bullough, P. A. The 8.5 Å Projection Structure of the Core RC-LH1-PufX Dimer of *Rhodobacter sphaeroides*. J. Mol. Biol. **2005**, 349, 948–960.

- (150) Koepke, J.; Hu, X.; Muenke, C.; Schulten, K.; Michel, H. The Crystal Structure of the Light Harvesting Complex II (B800-850) from *Rhodospirillum molischianum*. Structure **1996**, 4, 581–597.
- (151) McDermott, G.; Prince, S. M.; Freer, A. A.; Hawthornthwaite-Lawless, A. M.; Papiz, M. Z.; Cogdell, R. J.; Isaacs, N. W. Crystal structure of an integral membrane light-harvesting complex from photosynthetic bacteria. *Nature* 1995, 374, 517–521.
- (152) Papiz, M. Z.; Prince, S. M.; Howard, T.; Cogdell, R. J.; Isaacs, N. W. The structure and thermal motion of the B800-850 LH2 complex from *Rps. acidophila* at 2.0 Å resolution and 100 K: New structural features and functionally relevant motions. *J. Mol. Biol.* **2003**, *326*, 1523–1538.
- (153) Jamieson, S. J.; Wang, P.; Qian, P.; Kirkland, J. Y.; Conroy, M. J.; Hunter, C. N.; Bullough, P. A. Projection Structure of the photosynthetic reaction centre-antenna complex of *Rhodospirillum rubrum* at 8.5 Å resolution. *EMBO J.* 2002, 21, 3927–3935.
- (154) Hunter, C. N.; Kramer, H. J. M.; van Grondelle, R. Linear dichroism and fluorescence emission of antenna complexes during photosynthetic unit assembly in *Rhodopseudomonas sphaeroides*. *Biochim. Biophys. Acta* **1985**, *807*, 44–51.
- (155) Jackson, P. J.; Lewis, H. J.; Tucker, J. D.; Hunter, C. N.; Dickman, M. J. Quantitative proteomic analysis of intracytoplasmic membrane development in *Rhodobacter sphaeroides*. *Mol. Microbiol.* **2012**, *84*, 1062–1078.
- (156) Woronowicz, K.; Niederman, R. Proteomic analysis of the developing intracytoplasmic membrane in Rhodobacter sphaeroides during adaptation to low light intensity; Springer: New York, 2010; pp 161–178.
- (157) Woronowicz, K.; Harrold, J. W.; Kay, J. M.; Niederman, R. A. Structural and Functional Proteomics of Intracytoplasmic Membrane Assembly in *Rhodobacter sphaeroides*. *J. Mol. Microbiol. Biotech.* **2013**, *23*, 48–62.
- (158) Stone, J. E.; Sener, M.; Vandivort, K. L.; Barragan, A.; Singharoy, A.; Teo, I.; Ribeiro, J. V.; Isralewitz, B.; Liu, B.; Goh, B. C. et al. Atomic Detail Visualization of Photosynthetic Membranes with GPU-Accelerated Ray Tracing. *Parallel Computing* **2016**, *55*, 17–27.
- (159) Sener, M.; Stone, J. E.; Barragan, A.; Singharoy, A.; Teo, I.; Vandivort, K. L.; Isralewitz, B.; Liu, B.; Goh, B. C.; Phillips, J. C. et al. Visualization of Energy Conversion Processes in a Light Harvesting Organelle at Atomic Detail. Proceedings of the International Conference on High Performance Computing, Networking, Storage and Analysis. 2014; (4 pages).

- (160) Şener, M.; Schulten, K. A general random matrix approach to account for the effect of static disorder on the spectral properties of light harvesting systems. *Phys. Rev. E* **2002**, *65*, 031916, (12 pages).
- (161) Sener, M. K.; Hsin, J.; Trabuco, L. G.; Villa, E.; Qian, P.; Hunter, C. N.; Schulten, K. Structural model and excitonic properties of the dimeric RC-LH1-PufX complex from *Rhodobacter sphaeroides*. *Chem. Phys.* **2009**, *357*, 188–197.
- (162) Crofts, A. The cytochrome bc_1 complex: Function in the Context of Structure. Annu. Rev. Physiol. 2004, 66, 689–733.
- (163) Hakobyan, L.; Gabrielyan, L.; Trchounian, A. Relationship of proton motive force and the F(0)F(1)-ATPase with bio-hydrogen production activity of *Rhodobacter sphaeroides*: effects of diphenylene iodonium, hydrogenase inhibitor, and its solvent dimethylsulphoxide. *J Bioenerg. Biomembr.* **2012**, 44, 495–502.
- (164) Junge, W.; Nelson, N. ATP synthase. Ann. Rev. Biochem. 2015, 84, 631–657.
- (165) Noble, J. M.; Lubieniecki, J.; Savitzky, B. H.; Plitzko, J.; Engelhardt, H.; Baumeister, W.; Kourkoutis, L. F. Connectivity of centermost chromatophores in *Rhodobacter sphaeroides* bacteria. *Mol. Microbiol.* 2018, 109, 812–825.
- (166) Scholes, G. D.; Fleming, G. R.; Olaya-Castro, A.; Van Grondelle, R. Lessons from nature about solar light harvesting. *Nature chemistry* **2011**, *3*, 763–774.
- (167) Blankenship, R. E. Molecular mechanisms of photosynthesis; John Wiley & Sons, 2021.
- (168) R., M. D.; Matyushov., D. V. Photosynthetic diode: Electron transport rectification by wetting the quinone cofactor. *Physical Chemistry Chemical Physics* **2015**, *17*, 22523–22528.
- (169) Gisriel, C.; Sarrou, I.; Ferlez, B.; Golbeck, J. H.; Redding, K. E.; Fromme, R. Structure of a symmetric photosynthetic reaction center–photosystem. *Science* **2017**, *357*, 1021–1025.
- (170) Lavergne, J.; Verméglio, A.; Joliot, P. In *The Purple Phototrophic Bacteria*; Hunter, C. N., Daldal, F., Thurnauer, M. C., Beatty, J. T., Eds.; Springer, 2009; pp 509–536.
- (171) Niederman, R. A. Membrane development in purple photosynthetic bacteria in response to alterations in light intensity and oxygen tension. *Photosyn. Res.* **2013**, *116*, 333–48.
- (172) Scherf, M.; Scheffler, F.; Maffeo, C.; Kemper, U.; Ye, J.; Aksimentiev, A.; Seidel, R.; Reibetanz, U. Trapping of protein cargo molecules inside DNA origami nanocages. *Nanoscale* **2022**, *14*, 18041–18050.

- (173) Maffeo, C.; Chou, H.-Y.; Aksimentiev, A. Single-molecule biophysics experiments in silico: Toward a physical model of a replisome. *Iscience* **2022**, *25*, 104264.
- (174) Theis, T. N.; Wong, H.-S. P. The end of moore's law: A new beginning for information technology.

 *Computing in science & engineering 2017, 19, 41–50.
- (175) Phillips, J. C.; Braun, R.; Wang, W.; Gumbart, J.; Tajkhorshid, E.; Villa, E.; Chipot, C.; Skeel, R. D.; Kale, L.; Schulten, K. Scalable molecular dynamics with NAMD. *Journal of computational chemistry* **2005**, *26*, 1781–1802.
- (176) Souza, P. C.; Alessandri, R.; Barnoud, J.; Thallmair, S.; Faustino, I.; Grünewald, F.; Patmanidis, I.; Abdizadeh, H.; Bruininks, B. M.; Wassenaar, T. A. et al. Martini 3: a general purpose force field for coarse-grained molecular dynamics. *Nature methods* **2021**, *18*, 382–388.
- (177) Elgeti, J.; Winkler, R. G.; Gompper, G. Physics of microswimmers—single particle motion and collective behavior: a review. *Reports on progress in physics* **2015**, *78*, 056601.
- (178) Buttinoni, I.; Bialké, J.; Kümmel, F.; Löwen, H.; Bechinger, C.; Speck, T. Dynamical clustering and phase separation in suspensions of self-propelled colloidal particles. *Physical review letters* **2013**, *110*, 238301.
- (179) Paxton, W. F.; Kistler, K. C.; Olmeda, C. C.; Sen, A.; St. Angelo, S. K.; Cao, Y.; Mallouk, T. E.; Lammert, P. E.; Crespi, V. H. Catalytic nanomotors: autonomous movement of striped nanorods. *Journal of the American Chemical Society* **2004**, *126*, 13424–13431.
- (180) Howse, J. R.; Jones, R. A.; Ryan, A. J.; Gough, T.; Vafabakhsh, R.; Golestanian, R. Self-motile colloidal particles: from directed propulsion to random walk. *Physical review letters* **2007**, *99*, 048102.
- (181) Bickel, T.; Majee, A.; Würger, A. Flow pattern in the vicinity of self-propelling hot Janus particles.

 Physical Review E 2013, 88, 012301.
- (182) Maier, A. M.; Weig, C.; Oswald, P.; Frey, E.; Fischer, P.; Liedl, T. Magnetic propulsion of microswimmers with DNA-based flagellar bundles. *Nano letters* **2016**, *16*, 906–910.
- (183) Bechinger, C.; Di Leonardo, R.; Löwen, H.; Reichhardt, C.; Volpe, G.; Volpe, G. Active particles in complex and crowded environments. *Reviews of Modern Physics* **2016**, *88*, 045006.
- (184) Mathesh, M.; Wilson, D. A. Photosynthesis drives the motion of bio-nanomotors. *Advanced Intelligent Systems* **2020**, *2*, 2000028.

- (185) Reichert, J. Transport coefficients in dense active brownian particle systems. Ph.D. thesis, Dissertation, Düsseldorf, Heinrich-Heine-Universität, 2020, 2021.
- (186) MacGregor-Chatwin, C.; Jackson, P. J.; Sener, M.; Chidgey, J. W.; Hitchcock, A.; Qian, P.; Mayne-ord, G. E.; Johnson, M. P.; Luthey-Schulten, Z.; Dickman, M. J. et al. Membrane organization of photosystem I complexes in the most abundant phototroph on Earth. *Nature Plants* **2019**, *5*, 879–889.
- (187) MacGregor-Chatwin, C.; Sener, M.; Barnett, S. F.; Hitchcock, A.; Barnhart-Dailey, M. C.; Maghlaoui, K.; Barber, J.; Timlin, J. A.; Schulten, K.; Hunter, C. N. Lateral Segregation of Photosystem I in Cyanobacterial Thylakoid. *Plant Cell* **2017**, *29*, 1119–1136.
- (188) Amarnath, K.; Bennett, D. I.; Schneider, A. R.; Fleming, G. R. Multiscale model of light harvesting by photosystem II in plants. *Proceedings of the National Academy of Sciences* **2016**, *113*, 1156–1161.
- (189) Zhang, H.; Carey, A.-M.; Jeon, K.-W.; Liu, M.; Murrell, T. D.; Locsin, J.; Lin, S.; Yan, H.; Woodbury, N.; Seo, D.-K. A highly stable and scalable photosynthetic reaction center–graphene hybrid electrode system for biomimetic solar energy transduction. *Journal of Materials Chemistry A* **2017**, *5*, 6038–6041.
- (190) Merchuk, J. C.; Garcia-Camacho, F.; Molina-Grima, E. Photobioreactors-models of photosynthesis and related effects. *Comprehensive Biotechnology* **2019**, 320–360.
- (191) Gust, D. Why Study Photosynthesis? Center for Bioenergy & Photosynthesis. https://live-bioenergy. ws. asu. edu/content/why-study-photosynthesis 1996,
- (192) Alcorta, L.; Bazilian, M.; Simone, G. D.; Pedersen, A. Return on investment from industrial energy efficiency: evidence from developing countries. *Energ. Effic.* **2014**, *7*, 43–53.
- (193) Koolhaas, M.; Van der Zwan, G.; Frese, R.; Van Grondelle, R. Red shift of the zero crossing in the CD spectra of the LH2 antenna complex of Rhodopseudomonas acidophila: a structure-based study. *The Journal of Physical Chemistry B* **1997**, *101*, 7262–7270.
- (194) Rastogi, V. K.; Girvin, M. E. Structural changes linked to proton translocation by subunit c of the ATP synthase. *Nature* **1999**, *402*, 263–268.
- (195) Olkhova, E.; Hutter, M. C.; Lill, M. A.; Helms, V.; Michel, H. Dynamic water networks in cytochrome c oxidase from Paracoccus denitrificans investigated by molecular dynamics simulations. *Biophysical journal* **2004**, *86*, 1873–1889.
- (196) Riistama, S.; Hummer, G.; Puustinen, A.; Dyer, R. B.; Woodruff, W. H.; Wikström, M. Bound water in the proton translocation mechanism of the haem-copper oxidases. *FEBS letters* **1997**, *414*, 275–280.

- (197) Jemioła-Rzemińska, M.; Pasenkiewicz-Gierula, M.; Strzałka, K. The behavior of β-carotene in the phosphatidylcholine bilayer as revealed by a molecular simulation study. Chemistry and physics of lipids 2005, 135, 27–37.
- (198) Jeżowska, I.; Wolak, A.; Gruszecki, W. I.; Strzałka, K. Effect of β-carotene on structural and dynamic properties of model phosphatidylcholine membranes. II. A 31P-NMR and 13C-NMR study. Biochimica et Biophysica Acta (BBA)-Biomembranes 1994, 1194, 143–148.
- (199) Strzałka, K.; Gruszecki, W. I. Effect of β-carotene on structural and dynamic properties of model phosphatidylcholine membranes. I. An EPR spin label study. Biochimica et Biophysica Acta (BBA)-Biomembranes 1994, 1194, 138–142.
- (200) Vasil'ev, S.; Bruce, D. A protein dynamics study of photosystem II: the effects of protein conformation on reaction center function. *Biophysical Journal* **2006**, *90*, 3062–3073.
- (201) Raszewski, G.; Saenger, W.; Renger, T. Theory of optical spectra of photosystem II reaction centers: location of the triplet state and the identity of the primary electron donor. *Biophysical Journal* **2005**, *88*, 986–998.
- (202) Shen, G.; Eaton-Rye, J. J.; Vermaas, W. F. Mutation of histidine residues in CP47 leads to destabilization of the photosystem II complex and to impairment of light energy transfer. *Biochemistry* **1993**, *32*, 5109–5115.
- (203) Kokhan, O.; Wraight, C. A.; Tajkhorshid, E. The binding interface of cytochrome c and cytochrome c1 in the bc1 complex: rationalizing the role of key residues. *Biophysical journal* **2010**, *99*, 2647–2656.
- (204) Lange, C.; Hunte, C. Crystal structure of the yeast cytochrome bc 1 complex with its bound substrate cytochrome c. *Proceedings of the National Academy of Sciences* **2002**, *99*, 2800–2805.
- (205) Solmaz, S. R.; Hunte, C. Structure of complex III with bound cytochrome c in reduced state and definition of a minimal core interface for electron transfer. *Journal of biological chemistry* **2008**, *283*, 17542–17549.
- (206) Madeo, J.; Gunner, M. Modeling binding kinetics at the QA site in bacterial reaction centers. *Biochemistry* **2005**, *44*, 10994–11004.
- (207) Umena, Y.; Kawakami, K.; Shen, J.-R.; Kamiya, N. Crystal structure of oxygen-evolving photosystem II at a resolution of 1.9 Å. *Nature* **2011**, *473*, 55–60.
- (208) Schneider, A. R.; Geissler, P. L. Coexistence of fluid and crystalline phases of proteins in photosynthetic membranes. *Biophysical journal* **2013**, *105*, 1161–1170.

- (209) Kirchhoff, H.; Haase, W.; Wegner, S.; Danielsson, R.; Ackermann, R.; Albertsson, P.-A. Low-light-induced formation of semicrystalline photosystem II arrays in higher plant chloroplasts. *Biochemistry* **2007**, *46*, 11169–11176.
- (210) Kouřil, R.; Wientjes, E.; Bultema, J. B.; Croce, R.; Boekema, E. J. High-light vs. low-light: effect of light acclimation on photosystem II composition and organization in Arabidopsis thaliana. *Biochimica et Biophysica Acta (BBA)-Bioenergetics* **2013**, *1827*, 411–419.
- (211) Arnarez, C.; Mazat, J.-P.; Elezgaray, J.; Marrink, S.-J.; Periole, X. Evidence for Cardiolipin Binding Sites on the Membrane-Exposed Surface of the Cytochrome bc₁. *Journal of Biomolecular Structure and Dynamics* **2013**, *135*, 3112–3120.
- (212) Althoff, T.; Mills, D. J.; Popot, J.-L.; Kühlbrandt, W. Arrangement of electron transport chain components in bovine mitochondrial supercomplex I1III2IV1. *The EMBO journal* **2011**, *30*, 4652–4664.
- (213) Harris, B. J.; Cheng, X.; Frymier, P. All-atom molecular dynamics simulation of a photosystem i/detergent complex. *The Journal of Physical Chemistry B* **2014**, *118*, 11633–11645.
- (214) Lange, C.; Nett, J. H.; Trumpower, B. L.; Hunte, C. Specific roles of protein–phospholipid interactions in the yeast cytochrome bc1 complex structure. *The EMBO journal* **2001**, *20*, 6591–6600.
- (215) Fyfe, P. K.; Isaacs, N. W.; Cogdell, R. J.; Jones, M. R. Disruption of a specific molecular interaction with a bound lipid affects the thermal stability of the purple bacterial reaction centre. *Biochimica et Biophysica Acta (BBA)-Bioenergetics* **2004**, *1608*, 11–22.
- (216) Novoderezhkin, V. I.; Romero, E.; Dekker, J. P.; van Grondelle, R. Multiple charge-separation pathways in photosystem II: Modeling of transient absorption kinetics. *ChemPhysChem* **2011**, *12*, 681–688.
- (217) Lewis, K.; Fuller, F.; Myers, J.; Yocum, C.; Mukamel, S.; Abramavicius, D.; Ogilvie, J. Simulations of the two-dimensional electronic spectroscopy of the photosystem II reaction center. *The Journal of Physical Chemistry A* **2013**, *117*, 34–41.
- (218) Kaila, V. R.; Wikström, M.; Hummer, G. Electrostatics hydration and proton transfer dynamics in the membrane domain of respiratory complex I. Proceedings of the National Academy of Sciences 2014, 111, 6988–6993.
- (219) Freier, E.; Wolf, S.; Gerwert, K. Proton transfer via a transient linear water-molecule chain in a membrane protein. *The EMBO journal* **2011**, *108*, 11435–11439.

- (220) Liguori, N.; Periole, X.; Marrink, S. J.; Croce, R. From light-harvesting to photoprotection: structural basis of the dynamic switch of the major antenna complex of plants (LHCII). Scientific reports 2015, 5, 15661.
- (221) Dockter, C.; Müller, A. H.; Dietz, C.; Volkov, A.; Polyhach, Y.; Jeschke, G.; Paulsen, H. Rigid core and flexible terminus: structure of solubilized light-harvesting chlorophyll a/b complex (LHCII) measured by EPR. Journal of Biological Chemistry 2012, 287, 2915–2925.
- (222) Liu, Z.; Yan, H.; Wang, K.; Kuang, T.; Zhang, J.; Gui, L.; An, X.; Chang, W. Crystal structure of spinach major light-harvesting complex at 2.72 Å resolution. *Nature* **2004**, 428, 287–292.
- (223) Aviram, A.; Ratner, M. A. Molecular rectifiers. Chemical physics letters 1974, 29, 277–283.
- (224) Sharma, V.; Belevich, G.; Gamiz-Hernandez, A. P.; Róg, T.; Vattulainen, I.; Verkhovskaya, M. L.; Wikström, M.; Hummer, G.; Kaila, V. R. Redox-induced activation of the proton pump in the respiratory complex I. *Proceedings of the National Academy of Sciences* **2015**, *112*, 11571–11576.
- (225) Verkhovskaya, M.; Knuuti, J.; Wikström, M. Role of Ca²⁺ in structure and function of Complex I from Escherichia coli. *Biochimica et Biophysica Acta (BBA)-Bioenergetics* **2011**, *1807*, 36–41.
- (226) van Eerden, F. J.; de Jong, D. H.; de Vries, A. H.; Wassenaar, T. A.; Marrink, S. J. Characterization of thylakoid lipid membranes from cyanobacteria and higher plants by molecular dynamics simulations. Biochimica et Biophysica Acta (BBA)-Biomembranes 2015, 1848, 1319–1330.
- (227) Oliveira, A. S. F.; Campos, S. R.; Baptista, A. M.; Soares, C. M. Coupling between protonation and conformation in cytochrome c oxidase: Insights from constant-pH MD simulations. *Biochimica et Biophysica Acta (BBA)-Bioenergetics* **2016**, *1857*, 759–771.
- (228) Dinpajooh, M.; Martin, D. R.; Matyushov, D. V. Polarizability of the active site of cytochrome c reduces the activation barrier for electron transfer. *Scientific reports* **2016**, *6*, 28152.
- (229) Lockhart, D. J.; Boxer, S. G. Stark effect spectroscopy of Rhodobacter sphaeroides and Rhodopseudomonas viridis reaction centers. *Proceedings of the National Academy of Sciences* **1988**, *85*, 107–111.
- (230) Battistuzzi, G.; Borsari, M.; Bortolotti, C. A.; Di Rocco, G.; Ranieri, A.; Sola, M. Effects of mutational (Lys to Ala) surface charge changes on the redox properties of electrode-immobilized cytochrome c. *The Journal of Physical Chemistry B* **2007**, *111*, 10281–10287.

- (231) Wang, Y.; Cai, W.-S.; Chen, L.; Wang, G. Molecular dynamics simulation reveals how phosphorylation of tyrosine 26 of phosphoglycerate mutase 1 upregulates glycolysis and promotes tumor growth. *Oncotarget* **2017**, *8*, 12093.
- (232) Arai, S.; Saijo, S.; Suzuki, K.; Mizutani, K.; Kakinuma, Y.; Ishizuka-Katsura, Y.; Ohsawa, N.; Terada, T.; Shirouzu, M.; Yokoyama, S. et al. Rotation mechanism of Enterococcus hirae V1-ATPase based on asymmetric crystal structures. *Nature* **2013**, *493*, 703–707.
- (233) Mallus, M. I.; Shakya, Y.; Prajapati, J. D.; Kleinekathöfer, U. Environmental effects on the dynamics in the light-harvesting complexes LH2 and LH3 based on molecular simulations. *Chemical Physics* **2018**, 515, 141–151.
- (234) Qian, P.; Siebert, C. A.; Wang, P.; Canniffe, D. P.; Hunter, C. N. Cryo-EM structure of the Blastochloris viridis LH1–RC complex at 2.9 Å. *Nature* **2018**, *556*, 203–208.
- (235) Sarewicz, M.; Borek, A.; Daldal, F.; Froncisz, W.; Osyczka, A. Demonstration of short-lived complexes of cytochrome c with cytochrome bc1 by EPR spectroscopy: implications for the mechanism of interprotein electron transfer. *Journal of Biological Chemistry* **2008**, *283*, 24826–24836.
- (236) Hameedi, M. A.; Grba, D. N.; Richardson, K. H.; Jones, A. J.; Song, W.; Roessler, M. M.; Wright, J. J.; Hirst, J. A conserved arginine residue is critical for stabilizing the N2 FeS cluster in mitochondrial complex I. Journal of Biological Chemistry 2021, 296, 100474.
- (237) Khan, A.; Mohammad, T.; Shamsi, A.; Hussain, A.; Alajmi, M. F.; Husain, S. A.; Iqbal, M. A.; Hassan, M. I. Identification of plant-based hexokinase 2 inhibitors: Combined molecular docking and dynamics simulation studies. *Journal of Biomolecular Structure and Dynamics* **2022**, 40, 10319–10331.
- (238) Iida, T.; Minagawa, Y.; Ueno, H.; Kawai, F.; Murata, T.; Iino, R. Single-molecule analysis reveals rotational substeps and chemo-mechanical coupling scheme of Enterococcus hirae V1-ATPase. *Journal of Biological Chemistry* **2019**, *294*, 17017–17030.
- (239) Toei, M.; Noji, H. Single-molecule analysis of F0F1-ATP synthase inhibited by N, N-dicyclohexylcarbodiimide. *Journal of Biological Chemistry* **2013**, *288*, 25717–25726.